AD_____

Award Number:
W81XWH-08-1-0737

TITLE:
The Role of Phosphoinositide 3-Kinase in Breast Cancer

PRINCIPAL INVESTIGATOR:
Tina Yuan, PhD

CONTRACTING ORGANIZATION:
Harvard University
Boston, Massachusetts 02115

REPORT DATE:
October 2010

TYPE OF REPORT:
Annual Summary

PREPARED FOR: U.S. Army Medical Research and Materiel Command
Fort Detrick, Maryland 21702-5012

REPORT DOCUMENTATION PAGE

Form Approved
OMB No. 0704-0188

1. REPORT DATE *(DD-MM-YYYY)*	2. REPORT TYPE	3. DATES COVERED *(From - To)*
01-10-2010	Annual Summary	1 Oct 2008 - 30 Sep 2010

4. TITLE AND SUBTITLE

The Role of Phosphoinositide 3-kinase in Breast Cancer

5a. CONTRACT NUMBER

5b. GRANT NUMBER
W81XWH-08-1-0737

5c. PROGRAM ELEMENT NUMBER

6. AUTHOR(S)
Tina Yuan

5d. PROJECT NUMBER

5e. TASK NUMBER

5f. WORK UNIT NUMBER

7. PERFORMING ORGANIZATION NAME(S) AND ADDRESS(ES)

Harvard University
Boston, Massachusetts 02115

8. PERFORMING ORGANIZATION REPORT NUMBER

9. SPONSORING / MONITORING AGENCY NAME(S) AND ADDRESS(ES)
U.S. Army Medical Research and Material Command
Fort Detrick, Maryland 21702-5012

10. SPONSOR/MONITOR'S ACRONYM(S)

11. SPONSOR/MONITOR'S REPORT NUMBER(S)

12. DISTRIBUTION / AVAILABILITY STATEMENT

Approved for public release; distribution unlimited

13. SUPPLEMENTARY NOTES

14. ABSTRACT

Cell-to-cell variability in populations has been widely observed in mammalian cells. This heterogeneity can result from random stochastic events or can be deliberately maintained through regulatory processes. In the latter case, heterogeneity should confer a selective advantage that benefits the entire population. Using multicolor flow cytometry, we have uncovered robust heterogeneity in PI3K activity in MCF10A cell populations, which had been previously masked by techniques that only measure population averages. We show that AKT activity is bimodal in response to EGF stimulation and correlates with PI3K protein level, such that only cells with high PI3K protein can activate AKT. We further show that heterogeneity in PI3K protein levels is invariably maintained in cell populations through a degradation/re-synthesis cycle that can be regulated by cell density. Given that the PI3K pathway is one of the most frequently altered pathways in cancer, we propose that heterogeneity in PI3K activity is beneficial to normal tissues by restricting PI3K activation to only a subset of cells. This may serve to protect the population as a whole from over-activating the pathway, which can lead to cellular senescence or cancer.

15. SUBJECT TERMS
PI3K, AKT, heterogeneity

16. SECURITY CLASSIFICATION OF:			17. LIMITATION OF ABSTRACT	18. NUMBER OF PAGES	19a. NAME OF RESPONSIBLE PERSON
a. REPORT	b. ABSTRACT	c. THIS PAGE			USAMRMC
U	U	U	UU	64	19b. TELEPHONE NUMBER *(include area code)*

Table of Contents

Introduction

The phosphoinositide-3-kinase (PI3K) pathway regulates numerous critical cellular functions such as proliferation, growth and survival and is one of the most frequently altered pathways in human cancer [1]. Tumor cells have evolved numerous ways of over-activating this pathway to induce tumorigenesis, such as amplifications or mutations in upstream receptor tyrosine kinases (RTK), mutations or deletion of the negative regulator PTEN, somatic mutations in PI3K itself, and combinations of the above [2-4]. Nearly all of these genetic aberrations have been detected in breast carcinomas. This supports the notion that activation of the PI3K and the nodal kinase, protein kinase B (AKT/PKB), is a crucial element of mammary cell viability. However, it also implies that this pathway must be carefully regulated in order to prevent uncontrolled proliferation and survival that may lead to breast cancer.

Identification of these regulatory modules is critical to the development of novel treatments and to better inform our use of current therapies for breast cancers driven by PI3K signaling. We have now uncovered a previously uncharacterized mechanism to negatively regulate PI3K signaling in breast epithelial cell populations. We used an approach that analyzes signal transduction on the single cell level, which reveals population-context dependent regulatory networks that cannot be detected by more traditional analytical means such as western blots. Using multi-color flow cytometry, we demonstrate that MCF10A mammary cell populations invariably maintain heterogeneity in PI3K protein levels, characterized by a bimodal distribution of cells expressing either high or low levels of the enzyme. We further show that modulation of PI3K protein levels is regulated by proteosome-mediated degradation and *de novo* synthesis. This variability in PI3K protein levels subsequently leads to a bimodal distribution in downstream AKT activity. Our data lead us to hypothesize that heterogeneous PI3K/AKT activity is required to maintain low levels of PI3K activity in large cell populations in order to circumvent oncogenesis and senescence and respond to confluence arrest.

This work is builds on a growing body of work that characterizes cell-to-cell variability in cell populations. Ferrell and Machleder demonstrated that variability in MAPK phosphorylation leads to either a G2 or metaphase arrest in *Xenopus* oocytes [5]. Similarly, high or low levels of Nanog determines the potential of embryonic stem cells to terminally differentiate [6, 7], and high or low levels of Sca-1 dictates the proclivity for hematopoietic progenitor cells to commit to the erythroid or the myeloid lineage [8]. In certain epithelial cells, gefitinib-resistance can be conferred by high IGF-1R signaling and high KDM5A expression [9] and camptothecin-resistance by high DDX5 or RFC1 expression [10]. These studies shed much light on the importance of heterogeneous protein expression in the determination of distinct cellular fates. Our study now shows that heterogeneity in signal transduction is another meaningful source of cell-to-cell variability that results not in distinct cell fates, but rather influences the transient behavior of the entire population. This is particularly important in the context of tumor growth and the maintenance of homeostasis in tissues and organs.

Body

We present this body of work in its entirety in the Appendix A. We are pleased to report that it has recently been accepted for publication in *Current Biology* (Cell Press). The major findings are outlined briefly below. The first five findings were described in the previous Annual Summary, and the remaining three were completed in the time since the submission of the last Annual Summary.

AKT activation in MCF10A populations is heterogeneous and exhibits a bimodal distribution

Upon acute stimulation with EGF, we observed striking heterogeneity in AKT activation characterized by the bimodal distribution of cells into a pAKT-negative population (~70%) or a pAKT-positive population (~30%). Bimodality was also observed following insulin stimulation, suggesting that this is a general, rather than ligand-specific, effect on PI3K activation. We also observed robust bimodal activation of AKT in another non-transformed human mammary epithelial cell line, HMECs, but not in fully transformed breast cancer cell lines. This suggests that cancer cells have evolved a mechanism to overcome this negative regulation of AKT activation.

p110α protein level is variable in single cells and determines AKT activity

We found that p110α protein levels, like pAKT, exhibit bimodality in cell populations. p110α protein level also positively correlated with pAKT status ($R^2 = 0.68$), indicating that only cells with high levels of p110α can activate AKT. Additionally, levels of p85α mirror that of p110α in single cells, confirming that the entire holoenzyme is required to induce downstream signaling.

p110α protein levels are dynamic within single cells

We observed dynamic changes in p110α protein levels following EGF stimulation, which had not been previously reported. We show that p110α protein in pAKT-positive cells undergoes a precipitous drop 10 minutes after EGF stimulation, when AKT activity is maximal. In contrast, the major subgroup of cells with low levels of pAKT does not show a significant decline in p110α during the time course of EGF stimulation.

Dynamic changes in p110α protein levels are regulated by a degradation/re-synthesis cycle

We treated cells with the proteosome inhibitor, MG132, or the translation inhibitor, cyclohexamide, to monitor effects on p110α protein levels. We demonstrate that proteosome-mediated degradation of p110α transitions cells from the $p110\alpha^{high/medium}$ state to the $p110\alpha^{low}$ state, thereby negatively regulating AKT activity. Additionally, we show that p110α re-synthesis is responsible for shifting cells from the $p110\alpha^{low}$ state back to $p110\alpha^{high}$ state, thereby generating cells competent to activate AKT.

$p110\alpha^{high}$ cells initiate colony formation

We seeded single cells to generate clonal populations and show that early passage clones exhibit the reversed bimodal profile, characterized by a major proportion of cells with high levels of p110/pAKT and a small proportion of cells with low levels of p110/pAKT. These results suggest that only $p110\alpha^{high}$ cells were capable of forming colonies. Interestingly, as these clones were serially passaged, they all reverted back to the parental bimodal distribution. This suggests that $p110\alpha^{high}$ cells are critical for colony formation and early clonal expansion, however heterogeneous populations of

predominantly p110α^{low} cells facilitate exponential growth. Populations that fail to revert undergo senescence.

Hotspot *PIK3CA* mutations confer stabilization of the p110α^{high} state

We analyzed MCF10A cells expressing wildtype or either of two common oncogenic p110α mutants, H1047R and E545K. We show that the mutant proteins are maintained at higher concentrations in cells. This stability is partially conferred by a resistance to degradation and results in a greater proportion of cells with high levels of p110α, which ultimately leads to much higher levels of AKT activity within the population.

Establishing cell-cell contacts stabilizes the p110α^{low} state

We measured p110α levels of exponentially growing populations every 24h and found that p110α and pAKT levels steadily decreased as cell density increased. Under low-density growth conditions, the p110α^{high} population is enriched for cells with 0-1 cell-cell contacts, while the p110α^{low} population is enriched for cells with 2-4 cell-cell contacts. Thus, cell-cell contacts may modulate p110α levels in order to establish contact inhibition/confluence arrest.

AKT activity is enriched at the unencumbered edges of tumors

We stained mammary tumors arising from MMTV-Cre; BRCA1 flox/flox; p53+/- mice for pAKT S473. We detected heterogeneous pAKT-positivity throughout the tumor, including an enrichment of pAKT-positive cells along pushing margins and in the lumens of ductal hyperplasias. Both of these regions represent areas with fewer cell-cell contacts, supporting our hypothesis that low cell density enhances the pAKT-positive state.

Key Research Accomplishments

We have conducted an investigation of PI3K signaling in normal and cancer breast epithelial cell populations using multi-color flow cytometry. We have characterized a novel mechanism to negatively regulate PI3K signaling in cell populations that is based on the maintenance of variable PI3K protein expression. The key findings are:

- AKT activation in MCF10A populations is heterogeneous and exhibits a bimodal distribution
- p110α protein level is variable in single cells and determines AKT activity
- p110α protein levels are dynamic within single cells
- Dynamic changes in p110α protein levels are regulated by a degradation/re-synthesis cycle
- $p110\alpha^{high}$ cells initiate colony formation
- Hotspot *PIK3CA* mutations confer stabilization of the $p110\alpha^{high}$ state
- Establishing cell-cell contacts stabilizes the $p110\alpha^{low}$ state
- AKT activity is enriched at the unencumbered edges of tumors

Reportable Outcomes

During the funding period of this BCRP award, the following manuscripts have been published or have been accepted for publication:

1) Yuan, T.L., and Cantley, L.C. Introduction. Curr Top Microbiol Immunol *346*, 1-7.
2) Yuan, T.L., Wulf, G., Burga, L., and Cantley, L.C. (2011) Cell-to-cell variability in PI3K protein regulates PI3K-AKT pathway activity in cell populations. Curr Biol. ***Accepted.***

This work was presented in poster format at the 2010 Cold Spring Harbor James Watson Cancer Symposium.

This work has been presented in seminar format at Genentech and UCSF.

Conclusions

Single cell analysis of signal transduction networks can uncover many phenomena in cell populations that techniques that measure population averages cannot. Cell-to-cell heterogeneity is one such phenomenon. Heterogeneity can be the result of genetic or non-genetic variation and can have major effects on the behavior of the entire population. We have shown that heterogeneity in PI3K protein and pathway activation is an important mechanism in mammary epithelial cells to regulate growth in variable environmental contexts. Under acute growth factor stimulation, we show that heterogeneity results in AKT activation in only a subset of cells, which ensures that PI3K activity does not reach oncogenic levels. In low cell density conditions, we show that cells with high levels of PI3K are selected for colony formation and outgrowth, while under high density conditions, cells are maintained at the low PI3K state to dampen growth signals to perhaps to induce confluence arrest.

In cancer cells this negative regulation appears to be overcome. Cells expressing mutant forms of p110 appear to do this by stabilizing the PI3K enzyme, thus maintaining more actively signaling cells within the population. However, we showed that breast carcinomas derived from MMTV-Cre;BRCA1$^{flox/flox}$;p53$^{+/-}$ mice still maintain heterogeneity in AKT activation. There are likely to be many more AKT-positive cells than in normal breast tissue, however this remaining heterogeneity posits a major obstacle to the efficacy of PI3K inhibitors in the treatment of breast cancer.

It is likely that only tumor cells with high levels of pathway activation will die in response to acute inhibition of PI3K. Therefore, heterogeneous tumors will exhibit only “fractional killing” in response to a PI3K or AKT inhibitor. However, it may be possible to kill a larger fraction of the tumor cells by adjusting the therapy to ensure that the subset of cells that are protected from PI3K inhibitor therapy at the time of the initial dose, become exposed to the inhibitor a second time as they cycle into a high PI3K pathway state. Thus, a detailed understanding of the pharmacokinetics of the drug is important in deciding the intensity and frequency of dosing. While continuous high doses of PI3K inhibitors over several days or weeks might effectively kill all tumor cells as they cycle into the high activity state, dose-limiting toxicities might preclude such treatment.

A number of pre-clinical studies using PI3K inhibitors may support this hypothesis. Once daily oral administration of a PI3K inhibitor to tumor-bearing mice results in delayed tumor growth but rarely tumor regression. pAKT is ablated in these tumors 1-2h after dosing, but reemerges several hours later [11-15]. Our data would suggest that cells that were PI3K^{low};pAKT^{low} during the initial dose escaped the toxic effects of the drug, and cycled to the PI3K^{high};pAKT^{high} state several hours later when concentrations of the drug decreased. The possibility that PI3K inhibitors are selectively targeting the advancing edges or “pushing margins” of tumors is also consistent with fact that these tumors are not advancing, but rather stabilizing.

We believe that this work brings to light the need to carefully match the degree of tumor heterogeneity with the appropriate dosage of a drug in order to achieve sufficient tumor regression.

References

1. Cantley, L.C. (2002). The phosphoinositide 3-kinase pathway. Science *296*, 1655-1657.
2. Engelman, J.A. (2009). Targeting PI3K signalling in cancer: opportunities, challenges and limitations. Nat Rev Cancer *9*, 550-562.
3. Courtney, K.D., Corcoran, R.B., and Engelman, J.A. (2010). The PI3K pathway as drug target in human cancer. J Clin Oncol *28*, 1075-1083.
4. Yuan, T.L., and Cantley, L.C. (2008). PI3K pathway alterations in cancer: variations on a theme. Oncogene *27*, 5497-5510.
5. Ferrell, J.E., Jr., and Machleder, E.M. (1998). The biochemical basis of an all-or-none cell fate switch in Xenopus oocytes. Science *280*, 895-898.
6. Chambers, I., Silva, J., Colby, D., Nichols, J., Nijmeijer, B., Robertson, M., Vrana, J., Jones, K., Grotewold, L., and Smith, A. (2007). Nanog safeguards pluripotency and mediates germline development. Nature *450*, 1230-1234.
7. Kalmar, T., Lim, C., Hayward, P., Munoz-Descalzo, S., Nichols, J., Garcia-Ojalvo, J., and Martinez Arias, A. (2009). Regulated fluctuations in nanog expression mediate cell fate decisions in embryonic stem cells. PLoS Biol *7*, e1000149.
8. Chang, H.H., Hemberg, M., Barahona, M., Ingber, D.E., and Huang, S. (2008). Transcriptome-wide noise controls lineage choice in mammalian progenitor cells. Nature *453*, 544-547.
9. Sharma, S.V., Lee, D.Y., Li, B., Quinlan, M.P., Takahashi, F., Maheswaran, S., McDermott, U., Azizian, N., Zou, L., Fischbach, M.A., et al. (2010). A chromatin-mediated reversible drug-tolerant state in cancer cell subpopulations. Cell *141*, 69-80.
10. Cohen, A.A., Geva-Zatorsky, N., Eden, E., Frenkel-Morgenstern, M., Issaeva, I., Sigal, A., Milo, R., Cohen-Saidon, C., Liron, Y., Kam, Z., et al. (2008). Dynamic proteomics of individual cancer cells in response to a drug. Science *322*, 1511-1516.
11. Maira, S.M., Stauffer, F., Brueggen, J., Furet, P., Schnell, C., Fritsch, C., Brachmann, S., Chene, P., De Pover, A., Schoemaker, K., et al. (2008). Identification and characterization of NVP-BEZ235, a new orally available dual phosphatidylinositol 3-kinase/mammalian target of rapamycin inhibitor with potent in vivo antitumor activity. Mol Cancer Ther *7*, 1851-1863.
12. Cao, P., Maira, S.M., Garcia-Echeverria, C., and Hedley, D.W. (2009). Activity of a novel, dual PI3-kinase/mTor inhibitor NVP-BEZ235 against primary human pancreatic cancers grown as orthotopic xenografts. Br J Cancer *100*, 1267-1276.
13. Liu, T.J., Koul, D., LaFortune, T., Tiao, N., Shen, R.J., Maira, S.M., Garcia-Echevrria, C., and Yung, W.K. (2009). NVP-BEZ235, a novel dual phosphatidylinositol 3-kinase/mammalian target of rapamycin inhibitor, elicits multifaceted antitumor activities in human gliomas. Mol Cancer Ther *8*, 2204-2210.
14. Edgar, K.A., Wallin, J.J., Berry, M., Lee, L.B., Prior, W.W., Sampath, D., Friedman, L.S., and Belvin, M. (2010). Isoform-specific phosphoinositide 3-kinase inhibitors exert distinct effects in solid tumors. Cancer Res *70*, 1164-1172.
15. Raynaud, F.I., Eccles, S.A., Patel, S., Alix, S., Box, G., Chuckowree, I., Folkes, A., Gowan, S., De Haven Brandon, A., Di Stefano, F., et al. (2009). Biological properties of potent inhibitors of class I phosphatidylinositide 3-kinases: from PI-103 through PI-540, PI-620 to the oral agent GDC-0941. Mol Cancer Ther *8*, 1725-1738.

Appendix A

Accepted manuscript for “Cell-to-cell variability in PI3K protein regulates PI3K-AKT pathway activity in cell populations”

Cell-to-cell variability in PI3K protein level regulates PI3K-AKT pathway activity in cell populations

Tina L. Yuan[1,3,*], Gerburg Wulf[2,4], Laura Burga[2,4] and Lewis C. Cantley[1,3,5]

Department of Systems Biology[1] and Department of Medicine[2], Harvard Medical School, Boston, MA 02115; Division of Signal Transduction[3] and Division of Hematology and Oncology[4], Beth Israel Deaconess Medical Center, Boston, MA 02115

*Present address: Helen Diller Family Comprehensive Cancer Center, University of California, San Francisco, San Francisco, CA 94158

[5]Corresponding author: lewis_cantley@hms.harvard.edu

Summary

Background
Cell-to-cell variability in populations has been widely observed in mammalian cells. This heterogeneity can result from random stochastic events or can be deliberately maintained through regulatory processes. In the latter case, heterogeneity should confer a selective advantage that benefits the entire population.
Results
Using multicolor flow cytometry, we have uncovered robust heterogeneity in PI3K activity in MCF10A cell populations, which had been previously masked by techniques that only measure population averages. We show that AKT activity is bimodal in response to EGF stimulation and correlates with PI3K protein level, such that only cells with high PI3K protein can activate AKT. We further show that heterogeneity in PI3K protein levels is invariably maintained in cell populations through a degradation/re-synthesis cycle that can be regulated by cell density.
Conclusions
Given that the PI3K pathway is one of the most frequently altered pathways in cancer, we propose that heterogeneity in PI3K activity is beneficial to normal tissues by restricting PI3K activation to only a subset of cells. This may serve to protect the population as a whole from over-activating the pathway, which can lead to cellular senescence or cancer. Consistent with this, we show that oncogenic mutations in p110α (H1047R and E545K) partially evade this negative regulation, resulting in increased AKT activity in the population.

Highlights

- AKT activity in MCF10A populations is heterogeneous and is regulated by PI3K protein level
- Dynamic changes in PI3K protein levels are regulated by degradation and *de novo* translation
- Cells with high and low levels of PI3K protein have distinct cellular functions
- Oncogenic *PIK3CA* mutations stabilize high PI3K expression and induce high AKT activity

Introduction

Among the thousands of proteins expressed in a single cell at any one time, it is inevitable that even genetically identical cells will have variable expression of certain proteins. This cell-to-cell heterogeneity can have profound effects on the phenotype of a population. In bacteria and yeast, a heterogeneous population has a better chance of surviving in fluctuating environments [1-3]. In cancer cells, variable protein expression results in non-uniform responses to anti-cancer agents and only “fractional” killing, which is beneficial to the tumor but detrimental to the patient [4-7].

Population heterogeneity can be the result of genetic and non-genetic variability [8]. Non-genetic sources of heterogeneity are of particular interest because they are not fixed in the population by heritable transmission. Rather, these sources can be *stochastic* in nature, such as random fluctuations in transcription or translation, or they can be *regulated*, such as through feedback mechanisms, so that variability is deliberately maintained. Flow cytometry allows us to measure protein concentrations in single cells within large populations, which has proved useful in differentiating between stochastic and regulated sources of variation. Variable protein levels caused by stochastic events are usually rare and slightly increase the coefficient of variance (CV) of an otherwise log-normal concentration distribution [9]. Regulated variance usually deviates from tight log-normal distributions and in the most extreme cases might display bimodality [10]. Additionally, variance in the expression level of these proteins tend to correlate with variance in functionally related proteins [9].

We demonstrate cell-to-cell variability in phosphoinositide 3-kinase (PI3K) pathway activation in mammary epithelial cells that is indeed both bimodal and correlates with

multiple proteins in the pathway. This implies that heterogeneous PI3K activation in cell populations is maintained by a regulated process and likely confers a selective advantage. The PI3K pathway regulates numerous critical cellular functions such as proliferation, growth and survival and is one of the most frequently altered pathways in human cancer [11]. Tumor cells have evolved numerous ways of over-activating this pathway to induce tumorigenesis, such as amplifications or mutations in upstream receptor tyrosine kinases (RTK), mutations or deletion of the negative regulator PTEN, somatic mutations in PI3K itself, and combinations of the above [12-14]. In this view, we propose that cell-to-cell variability in PI3K activity serves as a mechanism to keep overall PI3K activity limited in normal tissues to avoid hyperactivity that may lead to cancer.

Results

AKT activation in MCF10A populations is heterogeneous and exhibits a bimodal distribution

To assess cell-to-cell variability in PI3K pathway activation, serum and growth factor starved MCF10A cells were acutely stimulated with EGF, and AKT activity was measured in single cells by flow cytometry. As expected, in the absence of EGF or with pretreatment with the PI3K inhibitor wortmannin, cells exhibited a log-normal distribution in the pAKT-negative gate (Figure 1A). Following treatment with saturating amounts of EGF, we observed striking heterogeneity in AKT activation characterized by the bimodal distribution of cells into the pAKT-negative (~70%) or pAKT-positive gates (~30%) (Figure 1A). The percentage of cells in the positive gate was maximal at 5-10 minutes and decreased over time. We found that the bimodality was not due to differential EGFR activation or total AKT protein abundance, both of which exhibit log-normal distributions and show weak correlation with pAKT status (Figure S1A,B). Bimodality was also observed following insulin stimulation, suggesting that this is a general, rather than ligand-specific, effect on PI3K activation (Figure S1C). We also observed robust bimodal activation of AKT in another non-transformed human mammary epithelial cell line, HMECs (Figure S1E).

As reported in the literature, cell populations expressing the oncogenic H1047R *PIK3CA* mutation have higher AKT activity [15-17]. The enzyme encoded by this mutant form of PIK3CA has been shown to have higher specific activity than that encoded by wild-type PIK3CA [15, 16]. To explore the possibility that this mutation shifts cells uniformly to the pAKT-positive state, MCF10A cells stably expressing this mutant form of p110α were

analyzed by flow cytometry. We observed that even in the presence of oncogenic p110α, cells still segregate into a bimodal distribution and retain a substantial population of non-responders. The H1047R mutation in MCF10A cells thus achieves higher average pAKT levels by shifting more cells into the pAKT-positive state (Figure 1A). This implies that the mechanism that maintains heterogeneity in cell populations is both robust and is not eliminated by expression of a mutant form of PI3K with constitutively high specific activity.

Lastly, we wanted to ensure that heterogeneous AKT activation is preserved in more physiological settings. Debnath *et al* have previously observed sporadic pAKT staining in MCF10A 3D acinar structures, which is important for proper lumen formation [18, 19]. To see if this heterogeneous AKT activation was observed *in vivo*, we analyzed spontaneously arising tumors from MMTV-Cre; BRCA1 flox/flox; p53+/- mice and indeed observed heterogeneity in pAKT positivity (Figure 1B).

p110α protein level is variable in single cells and determines AKT activity

Given that the bimodal AKT activation could not be explained by bimodal distribution of activated EGFR or total AKT protein, we next looked for variability in PI3K protein abundance. There are no p110α antibodies amenable for flow cytometry, however pAKT bimodality was maintained in MCF10A cells stably expressing HA-tagged p110α. We thus utilized anti-HA antibodies to monitor levels of p110α. Using single cell analysis, we found that p110α protein levels, like pAKT, exhibit bimodality in cell populations (Figure 1C). p110α protein level also positively correlated with pAKT status (R^2 = 0.68), indicating that only cells with high levels of p110α can activate AKT. Cells with medium levels of p110α have intermediate levels of AKT activity, suggesting that

these cells may be transitioning dynamically between the two dominant modes (Figure 1C). Subpopulations in these varying states can also be visualized by immunofluorescence (Figure 1D).

The p85α-p110α heterodimer is a very stable complex that does not readily dissociate, and it is thus thought that p110α levels generally correlate with p85α levels [20, 21]. We monitored the distribution of endogenous p85α in MCF10A cells and show that levels of endogenous p85α mirror that of HA-tagged p110α in single cells (Figure S1D). This correlation indicates that the heterogeneity we observe is not an artifact of exogenously expressed p110α and confirms that high levels of the entire functional holoenzyme are required for AKT activation, as expected.

p110α protein levels are dynamic within single cells

In agreement with previous studies [22-24], total PI3K levels do not appear to change upon growth factor stimulation as measured by western blot (Figure 2A). To test the possibility that p110α protein levels are dynamic on the subpopulation level, we measured p110α levels in pAKT-positive and pAKT-negative subpopulations over a time course of EGF stimulation by single cell analysis. Surprisingly, we observed dynamic changes in p110α protein in pAKT-positive cells. This minor subgroup of cells has the highest levels of p110α (and highest levels of pAKT) and undergoes a precipitous drop in p110α protein at 10 minutes after EGF stimulation, when AKT activity is maximal (Figure 2B). Over the next 4 hours, this population gradually recovers p110α levels (Figure 2B). In contrast, the major subgroup of cells with low levels of pAKT does not show a significant decline in p110α (and do not show activation of AKT) during the time

course of EGF stimulation. We attempted to verify these results with live cell imaging of fluorescently tagged p110α, however the size of the fluorescent protein-p110 fusion prohibited efficient transfection and expression.

However, our observed changes in p110α levels also correlate with a striking change in the proportion of cells in the $p110\alpha^{high}$, $p110\alpha^{medium}$, and $p110\alpha^{low}$ subpopulations over the time course of EGF stimulation. After 10 minutes of EGF stimulation, there is a major drop in the proportion of cells in the $p110\alpha^{high}$ state and an increase in the proportion of cells in the $p110\alpha^{medium}$ state (Figure 2C). Over the next 4 hours, the populations recover to the original distribution (Figure 2C). These data indicate that there is a significant decrease in p110α levels in a subpopulation of cells characterized by high pAKT and high p110α. The failure to detect this acute change in p110α by western blot can be explained by the fact that this population represents only a minor fraction of total cells, whereas the protein in a western blot is dominated by a major fraction of cells (70 to 80%) that fail to activate the PI3K/AKT pathway and maintain static p110α levels. Endogenous p85α levels exhibit nearly identical kinetics to p110α, indicating that the entire holoenzyme is dynamically regulated to modulate AKT activity (Figure S2).

We also plotted the time course of EGF-stimulated AKT phosphorylation in the sub-populations of cells that had high, medium or low levels of p110α (Figure 2D). The subset of cells with the highest level of p110α not only had the highest pAKT signal amplitude, but also the longest pAKT signal duration. However, the overall population response was dominated by the major subset of cells that had minimal AKT phosphorylation.

Dynamic changes in p110α protein levels are regulated by a degradation/re-synthesis cycle

We next sought to understand the mechanism by which p110α levels were modulated. In these cells, HA-p110α expression is driven by the CMV promoter, suggesting that variability in p110α expression is post-transcriptionally regulated. To test if the drop in p110α levels in actively signaling cells was due to proteosome-mediated degradation, we treated cells with MG132 and observed an increase in p110α protein on the population level (Figure 3A). On the subpopulation level, MG132 treatment resulted in the accumulation of cells in the $p110\alpha^{medium}$ state and a loss of cells from the $p110\alpha^{low}$ state (Figure 3B). This suggests that proteosome-mediated degradation of p110α transitions cells from the $p110\alpha^{high/medium}$ state to the $p110\alpha^{low}$ state, thereby negatively regulating AKT activity. Short-term treatment of cells with MG132 prior to acute EGF stimulation partially rescues the drop in p110 levels in pAKT high cells and prevents the shift of cells from the $p110\alpha^{high}$ to $p110\alpha^{medium}$ state (Figure S3A,B).

To show that p110α can be resynthesized and thus transition cells from the $p110\alpha^{low}$ to the $p110\alpha^{medium/high}$ state, we treated cells with cyclohexamide (CHX). On the population level, we observed an overall decrease in p110α protein with CHX treatment (Figure 3A). On the subpopulation level, we observed an accumulation of cells in the $p110\alpha^{low}$ state with concomitant loss of cells from the $p110\alpha^{medium}$ and $p110\alpha^{high}$ states (Figure 3B). These data show that p110α re-synthesis is responsible for shifting cells from the $p110\alpha^{low}$ state to $p110\alpha^{high}$ state, thereby generating cells competent to activate AKT.

Our results thus far suggest a model whereby p110α levels in single cells oscillate via a degradation/re-synthesis cycle, which transitions cells through phases of high p110α expression (competent to activate the pathway) and low p110α (incompetent to activate). Large populations contain cells in various stages of this cycle, thus accounting for the vast heterogeneity we observe (Figure 3C). Though many extrinsic factors are likely to influence the duration and progression of this cycle, we found no correlation between p110α or pAKT status with cell cycle, as assessed by DNA content, or with cell size or granularity (Table S1 and Figure S3C).

Hotspot *PIK3CA* mutations confer stabilization of the p110α^{high} state

Escaping this negative regulation of AKT may be particularly important in cancer cells, given that H1047R-expressing MCF10A cells and several tumor-derived breast cancer cell lines can activate AKT in a greater proportion of cells compared to non-transformed cell lines (Figures 1A, S1E). To test if this was due to the ability to stabilize the p110α^{high} state, we measured the level of p110α in MCF10A cells stably expressing exogenous HA-tagged wildtype, H1047R mutant, or E545K mutant p110α.

Both mutant forms of p110α were expressed at higher levels than wildtype p110α (Figure 4A), which was due to the maintenance of more cells in the p110α^{high} state and fewer cells in the p110α^{low} state (Figure 4B,C,H). To ensure that these differences were not due to variability in retroviral infection efficiency, multiple batches of cell lines were tested, and all lines were grown under selection for several generations before use in experiments.

We next sought to determine if the mutant forms of p110α were stabilizing the p110α^{high} state by resisting degradation. We monitored the degradation kinetics of the mutant cell lines as we did in Figure 2B. Though both mutant cell lines underwent rapid p110α degradation following EGF stimulation, the E545K mutant displayed more muted degradation (though this was, in part due to higher basal expression) and both mutants exhibited considerable variability between experiments compared to wildtype (Figure 4D). Additionally, MG132 treatment of asynchronously growing mutant cells did not result in an increase in overall p110α levels as observed in the wildtype line (Figure 4E). These results suggest that the H1047R and E545K mutations confer resistance to proteosome-mediated degradation under exponential growth conditions that may be distinct from the acute degradation that occurs following EGF stimulation of starved cells. Notably, all cell lines responded similarly upon CHX treatment, ruling out the possibility that mutant p110α is preferentially synthesized (Figure 4E).

To determine if stabilization of PI3K contributes to the oncogenic potential of the mutants, we compared overall AKT activity to total p110α levels in mutant and wildtype cells. During exponential growth, H1047R and E545K-expressing cells had 3.9 and 2.4-fold, respectively, more total AKT activity than those expressing wildtype PIK3CA, though the corresponding p110α levels were only 2.0 and 1.7-fold higher (Figure 4A,F,G). Given that these mutant forms of p110α are more enzymatically active [15, 16], we predict that the combination of more cells in the p110α^{high} state and higher enzymatic activity cooperate to induce oncogenic levels of AKT activity.

p110α^{high} cells initiate colony formation

We next investigated whether p110α^{high} cells had unique functional roles. We seeded single cells from wildtype, H1047R and E545K parental cell lines and generated clonal cell lines. Remarkably, nearly 100% of the clones that emerged exhibited a bimodal profile that was the reverse of the parental population. At early passage, the majority of cells were in the p110α^{high} state and a minority in the p110α^{low} state, with corresponding changes in pAKT (Figure 5A and Table S2). These results suggest that only p110α^{high} cells were capable of forming colonies, at least partially by maintaining high AKT activity. This is likely important for overcoming low cell density-related and replicative stresses, as we observed that cell lines over-expressing p110α, either wildtype or mutant, survived many more serial passages than clones with only endogenous levels of p110α (Figure 5B and Table S2).

If enrichment for p110α^{high} cells is important in the early stages of colony formation, we next wanted to test if the clones reverted back to the parental distribution once the population established steady exponential growth. We compared p110α levels at early and late passages and indeed saw reversion to the parental distribution with the majority of cells in the p110α^{low} state in late passages (Figure 5C). We carefully monitored the rate of reversion by measuring p110α levels in sequential passages and observed a gradual decrease in the percent of cells with high p110α in nearly all clones by passage 8 (Figure 5D). This suggests that p110α^{high} cells are critical for colony formation and early clonal expansion, however heterogeneous populations of predominantly p110α^{low} cells facilitate exponential growth. To ensure there was no genetic component to these effects, we established a second generation of clones from primary clonal populations and observed the same trends (Table S2). Additionally, reverted clonal cell lines

exhibited similar p110α kinetics after EGF stimulation to parental populations (Figure S4A-C).

Interestingly, at passage 3 both H1047R and E545K-derived clones harbored higher percentages of p110α^{high} cells compared to wildtype clones and reverted to the parental distribution at a slower rate than wildtype (Figure 5D). This is consistent with our previous observation that mutant p110α can stabilize the p110α^{high} state (Figure 4, S4D). Importantly, the few clones that failed to undergo a reversion to the parental distribution were predominantly mutant clones with very high percentages of p110α^{high} cells (Figure 5D). These clones ceased to proliferate after passage 3-4 and exhibited a spindly morphology and senescence-associated β-galactosidase activity (Figure 5E). We find these data consistent with a model where reversion to a bimodal distribution of primarily p110α^{low} cells is required to maintain exponential growth, and failure to revert results in oncogene-induced senescence.

Establishing cell-cell contacts stabilizes the p110α^{low} state.

If low cell density contributed to the induction of high p110α during colony formation, we wanted to explore the possibility that increasing cell-cell contacts induces the p110α^{low} state. We measured p110α levels of exponentially growing populations every 24h and found that p110α and pAKT levels steadily decreased as cell density increased (Figure 6A,B). The decrease in total p110α can be attributed specifically to a drop in the proportion p110α^{high} cells and an accumulation of p110α^{low} cells (Figure 6C). This is also apparent in small cell clusters, where p110α levels are heterogeneous compared to lone cells that tend to be p110α^{high} (Figure 6D). Under these low-density growth conditions,

the p110α^{high} population is enriched for cells with 0-1 cell-cell contacts, while the p110α^{low} population is enriched for cells with 2-4 cell-cell contacts (Figure 6D). Thus, cell-cell contacts may modulate p110α levels in order to establish contact inhibition/confluence arrest.

We next considered the possibility that cells with high AKT activity are enriched at the unencumbered edges of tumors, which are least confluence-inhibited and highly proliferative. These “pushing margins” are a distinct, though molecularly uncharacterized, feature of mutant *BRCA1*-driven tumors [25, 26]. We thus stained mammary tumors arising from MMTV-Cre; BRCA1 flox/flox; p53+/- mice for pAKT S473. We detected heterogeneous pAKT-positivity throughout the tumor (Figure S5A) and an enrichment of pAKT-positive cells along pushing margins (Figure S5B-F) and in the lumens of ductal hyperplasias (Figure S5G,H). Both of these regions represent areas with fewer cell-cell contacts, supporting our hypothesis that low cell density enhances the pAKT-positive state. However, given that no antibodies against p110α or p85α are amenable to immunohistochemical staining, we cannot confirm that this high AKT activity correlates with high PI3K protein.

Discussion

Non-genetic cell-to-cell variability has been observed in numerous cellular systems and can lead to distinct cellular fates. The most classic example is Ferrell and Machleder's study of *Xenopus* oocyte maturation, which shows that variability in MAPK phosphorylation leads to either a G2 or metaphase arrest [27]. Similarly, high or low levels of Nanog determines the potential of embryonic stem cells to terminally differentiate [10, 28], and high or low levels of Sca-1 dictates the proclivity for hemapotoietic progenitor cells to commit to the erythroid or the myeloid lineage [29]. Another cellular fate that is determined by variable protein expression is the drug-tolerant/drug-sensitive state. In certain cell lines, gefitinib-resistance can be conferred by high IGF-1R signaling and high KDM5A expression [7] and camptothecin-resistance by high DDX5 or RFC1 expression [4]. Our study now shows that heterogeneity in signal transduction is another meaningful source of cell-to-cell variability that results not in distinct cell fates, but rather influences the transient behavior of the entire population.

We show that a bimodal distribution of AKT activation is an invariable characteristic of exponentially growing MCF10A cells. We propose that limiting AKT activity to only 20-30% of cells in a population serves two related purposes: 1) to prevent senescence; and 2) to maintain sub-oncogenic levels of PI3K activity in large populations.

Our data show that clonal populations that are unable to revert to the parental distribution of primarily $p110\alpha^{low}$ cells undergo cellular senescence. In these clones, $p110\alpha^{high}$;$pAKT^{high}$ cells comprise 80-90% of the population immediately prior to senescence, indicating that such high PI3K activity is not sustainable. These results are consistent with models of p53-dependent cellular senescence associated with the loss of

two negative regulators of PI3K, PTEN and inositol polyphosphate 4-phosphatase type II (INPP4B) [30, 31]. Given that MCF10A cells are p53-replete, it is possible that over-accumulation of $p110\alpha^{high}$ cells induces senescence by the same mechanism.

A second selective advantage of maintaining variability in PI3K activity may be to maintain sub-oncogenic levels of PI3K activity in large populations such as tissues and organs. Given that over-activation of this pathway is one of the most frequent events in cancer, permitting PI3K activation in only a fraction of cells within a population may be a simple mechanism to limit overall PI3K activity. However, we show that variability is not completely overcome in populations expressing oncogenic forms of $p110\alpha$ or in epithelial tumor sections, which may have important implications on tumor susceptibility to PI3K inhibitors.

Assuming that only tumor cells with high levels of pathway activation are likely to die in response to acute inhibition of PI3K, then tumors with mosaic patterns of pathway activation (e.g. as judged by pAKT staining) will exhibit only a partial response to a PI3K (or AKT) inhibitor. The mosaic pattern of pathway activation could be due to genetic variability or oscillation between high and low levels of PI3K expression (as seen in MCF10A cells). In the latter case, it may be possible to kill a larger fraction of the tumor cells by adjusting the therapy to ensure that the subset of cells that are protected from PI3K inhibitor therapy at the time of the initial dose, become exposed to the inhibitor a second time as they cycle into a high PI3K pathway state. Thus, a detailed understanding of the pharmacokinetics of the drug is important in deciding the intensity and frequency of dosing. While continuous high doses of PI3K inhibitors over several days or weeks might effectively kill all tumor cells as they cycle into the high activity state, dose-limiting toxicities might preclude such treatment. An alternative approach of

using a very high single dose once a week could avoid toxicities associated with continuous dosing and result in 20-30% tumor cell death at the first treatment, followed by a period in which another 20-30% of the resistant tumor cells cycle into the high PI3K pathway state and die at the second treatment and etc.

Various pre-clinical studies using PI3K inhibitors may support this hypothesis. Once daily oral administration of the Novartis pan-PI3K/mTOR inhibitor, NVP-BEZ235, to tumor-bearing mice results in delayed tumor growth but rarely tumor regression. pAKT is ablated in these tumors 1-2h after dosing, but reemerges several hours later [32-34]. Similar results were observed using the Genentech class 1A PI3K inhibitor, GDC-0941 [35, 36]. Our data would suggest that cells that were $PI3K^{low}$;$pAKT^{low}$ during the initial dose escaped the toxic effects of the drug, and cycled to the $PI3K^{high}$;$pAKT^{high}$ state several hours later when concentrations of the drug decreased. The possibility that PI3K inhibitors are selectively targeting the advancing edges or “pushing margins” of tumors is also consistent with fact that these tumors are not advancing, but rather stabilizing.

As we emphasized throughout this study, variability in PI3K activity in cell populations is a regulated process. Though the mechanism regulating PI3K degradation and re-synthesis is beyond the scope of this study, it is tempting to consider inhibition of re-synthesis to dampen PI3K activity in all cells. Another alternative is to inhibit the E3 ligase that targets PI3K for degradation, which may over-activate the pathway in all cells and induce cellular senescence. This “pro-senescence” approach has recently shown promise in a prostate cancer xenograft model where PTEN is pharmacologically inhibited [37].

Materials and Methods

Cell lines and cell culture

MCF10A cells were obtained from the American Type Culture Collection and cultured as described by Debnath *et al* [38]. Stable MCF10A cell lines expressing HA-tagged wildtype or mutant (H1047R or E545K) bovine p110α were generated by retroviral infection as previously described [15]. Expression of wildtype and mutant PIK3CA cDNA was driven by the exogenous CMV promoter of the JP1520 retroviral vector (J. Pearlberg). Where indicated, cells were starved in growth media without horse serum, EGF or insulin for ~20h. Acute stimulation with growth factors was done by adding growth factor directly to the starvation medium.

Preparation of cells for flow cytometry

A detailed description of how to prepare adherent cells for analysis by flow cytometry is provided in the Supplemental Information. Antibodies used for flow cytometry were: anti-HA.11-488 conjugate (Covance); anti-p-AKT S473 (D9E)-488/647 conjugates, anti-total AKT-647 conjugate, anti-pEGFR Y1068 (Cell Signaling); anti-p85α (Upstate Biotechnology); and various secondary Alexa Fluor dyes (Invitrogen). Data was analyzed with BD FACSDiva software (BD Biosciences), FlowJo software (Tree Star) and Cytobank [39].

Generation of clonal populations

Parental pooled populations were passaged >9 times in selection media to normalize for infection efficiency. Parental cells were trypsinized, diluted and plated at a density of 1 cell/well. Colony formation was monitored daily and media was changed every three

days. Once colonies grew to a sufficient size, they were trypsinized and re-plated (passage 1) and serially passaged thereafter.

Immunoassays

Detailed protocols for immunofluorescence, immunoblotting, and immunohistochemistry are provided in the Supplemental Information.

Figure Legends

Figure 1. PI3K pathway activation in MCF10A populations is heterogeneous.

(A) Cells were starved and acutely stimulated with 5nM EGF for 5' with or without pretreatment with 100nM wortmannin. Cells were then harvested and stained with anti-pAKT S473 antibody and analyzed by flow cytometry. Unstimulated and wortmannin treated cells are pAKT-negative (P6). EGF stimulation activates ~30% of cells and shifts them into the pAKT-positive gate (P7). Cells stably expressing the oncogenic H1047R p110α mutant exhibit basal AKT activity in the unstimulated state (as previously reported), and EGF stimulation shifts more cells into the pAKT-positive gate (P7) as well as increases the amplitude of pAKT signal (P8).

(B) Mammary carcinomas from MMTV-Cre; BRCA1flox/flox; p53+/- mice display heterogeneous pAKT-positivity.

(C) MCF10A cells stably expressing HA-tagged p110α were treated as described in (A) and co-stained with anti-pAKT S473 and anti-HA antibodies. HA-p110α segregates into a bimodal distribution and correlates with pAKT status (R^2=0.68).

(D) The results from (C) were validated by immunofluorescence.

Figure 2. p110α levels are dynamic within single cells.

(A) MCF10A cells stably expressing wildtype HA-p110α were starved and acutely stimulated with 5nM EGF. Cell lysates were harvested at indicated time points and analyzed by SDS-PAGE.

(B) MCF10A cells stably expressing wildtype HA-p110α were treated as described in (A). Cells were harvested at indicated time points and analyzed by flow cytometry. The average p110α level in the population (solid blue line) remains low and unchanging, as seen by western blot in (A). On the subpopulation level, pAKT-positive cells (solid red line) initially have high levels of p110α, which drop precipitously at 10' and recover over time. The pAKT-negative subpopulation (dotted red line) retains constant low levels of p110α. The dynamic changes in p110α levels in the pAKT-positive subpopulation can modestly influence p110α levels of the entire population, as seen by the slight increase in p110α in the presence of MG132 (dotted blue line).

(C) The proportion of cells in the $p110\alpha^{high/medium/low}$ gates was measured at each time point in a representative experiment described in (B). Fold change compared to time 0 is shown, indicating a shift of cells from the $p110\alpha^{high}$ to $p110\alpha^{medium}$ to $p110\alpha^{low}$ states and back. The short 4h time course ensures that these dynamic changes are not due to cell division.

(D) Average AKT activity was measured on the population and subpopulation levels in the cells from (B). $p110\alpha^{high}$ cells (solid black line) maximally activate AKT compared to $p110\alpha^{low}$ cells (dashed black line), which minimally activate AKT. $p110\alpha^{medium}$ cells (dotted black line) have intermediate levels of pAKT. Given that the $p110\alpha^{high}$ cells only represent ~30% of the population, the average pAKT

level on the population level (red line) is only slightly higher than the p110α^{low} line.

Figure 3. Changes in p110α levels are regulated by a degradation/re-synthesis cycle.

(A) Asynchronously growing MCF10A cells expressing wildtype HA-p110α were treated for 4h with 100μg/mL cyclohexamide (CHX) or 20μM MG132 and analyzed by flow cytometry. (Left panel) On the population level, CHX (blue line) and MG132 (orange line) treatment shifted the p110α distribution to the left and right, respectively, compared to untreated cells (green line). (Right panel) These shifts in p110α levels correlate with changes in overall pAKT level.

(B) On the subpopulation level, CHX treatment inhibits the accumulation of cells in the p110α$^{medium/high}$ gates by retaining cells in the p110α^{low} state. MG132 treatment results in the accumulation of cells in the p110α$^{medium/high}$ gates. Changes in population distribution are quantified in the right panel.

(C) Model of PI3K degradation/re-synthesis cycle that regulates pathway activation. (Left panel) Inactive cells are p110α^{low}; pAKT^{low} (Q4). Extrinsic signals trigger *de novo* synthesis of PI3K protein, transitioning cells to a p110α^{high}; pAKT^{low} state (Q1), where they are competent to activate the pathway. Once a growth signal is received, cells transition to the p110α^{high}; pAKT^{high} state (Q2) and the PI3K pathway is fully activated. Shortly after activation, PI3K is rapidly degraded and

cells enter the p110α^{low}; pAKT^{high} state (Q3). Once AKT is fully dephosphorylated, cells return to the inactive (Q4) state. (Right panel) Immunofluorescence of EGF stimulated cells shows cells in each of these four stages of the cycle.

Figure 4. *PIK3CA* mutations stabilize the p110α^{high} state.

(A) Asynchronously growing MCF10A cells stably expressing HA-tagged wildtype or mutant p110α (H1047R or E545K) were analyzed by flow cytometry. Cells expressing the H1047R or E545K mutations had 2.0 and 1.7-fold, respectively, higher levels of p110α compared to wildtype.

(B) The proportion of cells within the p110α$^{high/medium/low}$ gates was measured for the three cell lines. Both mutant cell lines had more cells with high levels of p110α and fewer cells with low levels of p110α.

(C) Asynchronously growing cells expressing wildtype p110α only have ~25% of cells actively signaling or primed to activate signaling compared to >40% in either mutant cell line. Numbers represent an average of three experiments.

(D) Cells expressing wildtype or mutant p110α were treated as described in Figure 2B. Total levels of p110α in the whole population did not change over time (solid lines), though the mutant cells retained higher average p110α levels than the wildtype cells. In the pAKT^{high} subpopulations (dashed lines), the mutants followed similar dynamic changes in p110α levels as described for wildtype, though with much greater variability.

(E) Asynchronously growing wildtype and mutant lines were treated with CHX or MG132 as described in Figure 3A. All cell lines showed a decrease in p110α levels following treatment with CHX. However the mutant lines were less sensitive to the MG132 treatment than the wildtype line.

(F) Average AKT activity in asynchronously growing wildtype and mutant cell populations was measured by flow cytometry. The H1047R and E545K mutant lines exhibited 3.9 and 2.4-fold increases, respectively, in total pAKT level compared to wildtype.

(G) Wildtype and mutant cells were analyzed by immunofluorescence as described in Figure 1.

Figure 5. Cells with high levels of p110α are important for colony formation.

(A) On passage 3, clonal cell lines were starved and acutely stimulated with 5nM EGF and analyzed by flow cytometry. In each set of histograms, the top (blue) measures p110α and the bottom measures pAKT S473 of $p110\alpha^{low}$ (green) and $p110\alpha^{high}$ (red) cells.

(B) Clones over-expressing wildtype or mutant p110α survived more passages than cells with only endogenous levels of p110α. Additionally, expression of either

mutant form of p110α increased clonal viability at early passages compared to expression of wildtype p110α.

(C) Clones at late passage (>10) were analyzed as described in (A) and invariably reverted to the parental bimodal distribution characterized by a large $p110\alpha^{low}$ subpopulation and a small $p110\alpha^{high}$ subpopulation.

(D) To monitor the rate of reversion, the percent of cells with high levels of p110α was measured by flow cytometry for six serial passages. Mutant clones (middle and bottom) achieved higher $p110\alpha^{high}$ percentages and reverted slower than wildtype clones (top). Notably, many mutant clones (HR-5,6,7 and EK-10,8,11,14) failed to revert and instead ceased proliferating at early passage.

(E) Clones that stopped growing stained positively for senescence-associated β-galactosidase activity compared to an exponentially growing control line.

Figure 6. Establishing cell-cell contacts stabilizes the $p110\alpha^{low}$ state.

(A) Cells achieve ~1.5 doublings every 24h, thereby increasing the number of cell-cell contacts.

(B) Asynchronously growing cells were harvested every 24h and analyzed by flow cytometry. As cell density increases, average p110α (left) and pAKT (right)

levels in the population decreases. Data shown are from one representative experiment.

(C) Analyzed on the subpopulation level, the decrease in p110α can be attributed specifically to a decrease in the p110α^{high} subpopulation and an accumulation of the p110α^{low} subpopulation.

(D) To verify these results, cells were grown to ~50% confluency and p110α levels were assessed by immunofluorescence (Left panel). Cells with few or no cell-cell contacts (white circles) stained brightly for HA-p110α whereas cell clusters with many cell-cell contacts (orange boxes) displayed heterogeneity in HA-p110α staining intensity. The number of cell-cell contacts was counted for 875 individual cells and compared to their p110α status (Right panel). p110α^{high} cells were enriched for cells with 0-1 cell-cell contacts and p110α^{low} cells were enriched for cells with 2-4 cell-cell contacts.

Acknowledgements

We thank Jeffrey Engelman for providing us with the *PIK3CA* retroviral constructs and Kevin Courtney and Cyril Benes for insightful discussions. This work is funded by the Department of Defense Breast Cancer Research Program award W81XWH-08-1-0737 (to T.L.Y.), National Institutes of Health grant R01GM41890-21 (to L.C.C.) and Susan Komen Foundation grant BCTR0601030 and the Department of Defense Concept Award BC 046321 (to G.W.).

References

1. Balaban, N.Q., Merrin, J., Chait, R., Kowalik, L., and Leibler, S. (2004). Bacterial persistence as a phenotypic switch. Science *305*, 1622-1625.
2. Acar, M., Mettetal, J.T., and van Oudenaarden, A. (2008). Stochastic switching as a survival strategy in fluctuating environments. Nat Genet *40*, 471-475.
3. Raj, A., and van Oudenaarden, A. (2008). Nature, nurture, or chance: stochastic gene expression and its consequences. Cell *135*, 216-226.
4. Cohen, A.A., Geva-Zatorsky, N., Eden, E., Frenkel-Morgenstern, M., Issaeva, I., Sigal, A., Milo, R., Cohen-Saidon, C., Liron, Y., Kam, Z., et al. (2008). Dynamic proteomics of individual cancer cells in response to a drug. Science *322*, 1511-1516.
5. Spencer, S.L., Gaudet, S., Albeck, J.G., Burke, J.M., and Sorger, P.K. (2009). Non-genetic origins of cell-to-cell variability in TRAIL-induced apoptosis. Nature *459*, 428-432.
6. Gascoigne, K.E., and Taylor, S.S. (2008). Cancer cells display profound intra- and interline variation following prolonged exposure to antimitotic drugs. Cancer Cell *14*, 111-122.
7. Sharma, S.V., Lee, D.Y., Li, B., Quinlan, M.P., Takahashi, F., Maheswaran, S., McDermott, U., Azizian, N., Zou, L., Fischbach, M.A., et al. (2010). A chromatin-mediated reversible drug-tolerant state in cancer cell subpopulations. Cell *141*, 69-80.
8. Huang, S. (2009). Non-genetic heterogeneity of cells in development: more than just noise. Development *136*, 3853-3862.
9. Niepel, M., Spencer, S.L., and Sorger, P.K. (2009). Non-genetic cell-to-cell variability and the consequences for pharmacology. Curr Opin Chem Biol *13*, 556-561.
10. Kalmar, T., Lim, C., Hayward, P., Munoz-Descalzo, S., Nichols, J., Garcia-Ojalvo, J., and Martinez Arias, A. (2009). Regulated fluctuations in nanog expression mediate cell fate decisions in embryonic stem cells. PLoS Biol *7*, e1000149.
11. Cantley, L.C. (2002). The phosphoinositide 3-kinase pathway. Science *296*, 1655-1657.
12. Engelman, J.A. (2009). Targeting PI3K signalling in cancer: opportunities, challenges and limitations. Nat Rev Cancer *9*, 550-562.
13. Courtney, K.D., Corcoran, R.B., and Engelman, J.A. (2010). The PI3K pathway as drug target in human cancer. J Clin Oncol *28*, 1075-1083.
14. Yuan, T.L., and Cantley, L.C. (2008). PI3K pathway alterations in cancer: variations on a theme. Oncogene *27*, 5497-5510.
15. Isakoff, S.J., Engelman, J.A., Irie, H.Y., Luo, J., Brachmann, S.M., Pearline, R.V., Cantley, L.C., and Brugge, J.S. (2005). Breast cancer-associated PIK3CA mutations are oncogenic in mammary epithelial cells. Cancer Res *65*, 10992-11000.
16. Kang, S., Bader, A.G., and Vogt, P.K. (2005). Phosphatidylinositol 3-kinase mutations identified in human cancer are oncogenic. Proc Natl Acad Sci U S A *102*, 802-807.
17. Samuels, Y., Diaz, L.A., Jr., Schmidt-Kittler, O., Cummins, J.M., Delong, L., Cheong, I., Rago, C., Huso, D.L., Lengauer, C., Kinzler, K.W., et al. (2005). Mutant PIK3CA promotes cell growth and invasion of human cancer cells. Cancer Cell *7*, 561-573.

18. Debnath, J., Mills, K.R., Collins, N.L., Reginato, M.J., Muthuswamy, S.K., and Brugge, J.S. (2002). The role of apoptosis in creating and maintaining luminal space within normal and oncogene-expressing mammary acini. Cell *111*, 29-40.
19. Debnath, J., Walker, S.J., and Brugge, J.S. (2003). Akt activation disrupts mammary acinar architecture and enhances proliferation in an mTOR-dependent manner. J Cell Biol *163*, 315-326.
20. Brachmann, S.M., Ueki, K., Engelman, J.A., Kahn, R.C., and Cantley, L.C. (2005). Phosphoinositide 3-kinase catalytic subunit deletion and regulatory subunit deletion have opposite effects on insulin sensitivity in mice. Mol Cell Biol *25*, 1596-1607.
21. Ueki, K., Fruman, D.A., Brachmann, S.M., Tseng, Y.H., Cantley, L.C., and Kahn, C.R. (2002). Molecular balance between the regulatory and catalytic subunits of phosphoinositide 3-kinase regulates cell signaling and survival. Mol Cell Biol *22*, 965-977.
22. Luo, J., Field, S.J., Lee, J.Y., Engelman, J.A., and Cantley, L.C. (2005). The p85 regulatory subunit of phosphoinositide 3-kinase down-regulates IRS-1 signaling via the formation of a sequestration complex. J Cell Biol *170*, 455-464.
23. Taniguchi, C.M., Aleman, J.O., Ueki, K., Luo, J., Asano, T., Kaneto, H., Stephanopoulos, G., Cantley, L.C., and Kahn, C.R. (2007). The p85alpha regulatory subunit of phosphoinositide 3-kinase potentiates c-Jun N-terminal kinase-mediated insulin resistance. Mol Cell Biol *27*, 2830-2840.
24. Ueki, K., Fruman, D.A., Yballe, C.M., Fasshauer, M., Klein, J., Asano, T., Cantley, L.C., and Kahn, C.R. (2003). Positive and negative roles of p85 alpha and p85 beta regulatory subunits of phosphoinositide 3-kinase in insulin signaling. J Biol Chem *278*, 48453-48466.
25. Lakhani, S.R., Jacquemier, J., Sloane, J.P., Gusterson, B.A., Anderson, T.J., van de Vijver, M.J., Farid, L.M., Venter, D., Antoniou, A., Storfer-Isser, A., et al. (1998). Multifactorial analysis of differences between sporadic breast cancers and cancers involving BRCA1 and BRCA2 mutations. J Natl Cancer Inst *90*, 1138-1145.
26. Liu, X., Holstege, H., van der Gulden, H., Treur-Mulder, M., Zevenhoven, J., Velds, A., Kerkhoven, R.M., van Vliet, M.H., Wessels, L.F., Peterse, J.L., et al. (2007). Somatic loss of BRCA1 and p53 in mice induces mammary tumors with features of human BRCA1-mutated basal-like breast cancer. Proc Natl Acad Sci U S A *104*, 12111-12116.
27. Ferrell, J.E., Jr., and Machleder, E.M. (1998). The biochemical basis of an all-or-none cell fate switch in Xenopus oocytes. Science *280*, 895-898.
28. Chambers, I., Silva, J., Colby, D., Nichols, J., Nijmeijer, B., Robertson, M., Vrana, J., Jones, K., Grotewold, L., and Smith, A. (2007). Nanog safeguards pluripotency and mediates germline development. Nature *450*, 1230-1234.
29. Chang, H.H., Hemberg, M., Barahona, M., Ingber, D.E., and Huang, S. (2008). Transcriptome-wide noise controls lineage choice in mammalian progenitor cells. Nature *453*, 544-547.
30. Chen, Z., Trotman, L.C., Shaffer, D., Lin, H.K., Dotan, Z.A., Niki, M., Koutcher, J.A., Scher, H.I., Ludwig, T., Gerald, W., et al. (2005). Crucial role of p53-dependent cellular senescence in suppression of Pten-deficient tumorigenesis. Nature *436*, 725-730.
31. Gewinner, C., Wang, Z.C., Richardson, A., Teruya-Feldstein, J., Etemadmoghadam, D., Bowtell, D., Barretina, J., Lin, W.M., Rameh, L., Salmena, L., et al. (2009). Evidence that inositol polyphosphate 4-phosphatase

type II is a tumor suppressor that inhibits PI3K signaling. Cancer Cell *16*, 115-125.
32. Maira, S.M., Stauffer, F., Brueggen, J., Furet, P., Schnell, C., Fritsch, C., Brachmann, S., Chene, P., De Pover, A., Schoemaker, K., et al. (2008). Identification and characterization of NVP-BEZ235, a new orally available dual phosphatidylinositol 3-kinase/mammalian target of rapamycin inhibitor with potent in vivo antitumor activity. Mol Cancer Ther *7*, 1851-1863.
33. Cao, P., Maira, S.M., Garcia-Echeverria, C., and Hedley, D.W. (2009). Activity of a novel, dual PI3-kinase/mTor inhibitor NVP-BEZ235 against primary human pancreatic cancers grown as orthotopic xenografts. Br J Cancer *100*, 1267-1276.
34. Liu, T.J., Koul, D., LaFortune, T., Tiao, N., Shen, R.J., Maira, S.M., Garcia-Echevrria, C., and Yung, W.K. (2009). NVP-BEZ235, a novel dual phosphatidylinositol 3-kinase/mammalian target of rapamycin inhibitor, elicits multifaceted antitumor activities in human gliomas. Mol Cancer Ther *8*, 2204-2210.
35. Edgar, K.A., Wallin, J.J., Berry, M., Lee, L.B., Prior, W.W., Sampath, D., Friedman, L.S., and Belvin, M. (2010). Isoform-specific phosphoinositide 3-kinase inhibitors exert distinct effects in solid tumors. Cancer Res *70*, 1164-1172.
36. Raynaud, F.I., Eccles, S.A., Patel, S., Alix, S., Box, G., Chuckowree, I., Folkes, A., Gowan, S., De Haven Brandon, A., Di Stefano, F., et al. (2009). Biological properties of potent inhibitors of class I phosphatidylinositide 3-kinases: from PI-103 through PI-540, PI-620 to the oral agent GDC-0941. Mol Cancer Ther *8*, 1725-1738.
37. Alimonti, A., Nardella, C., Chen, Z., Clohessy, J.G., Carracedo, A., Trotman, L.C., Cheng, K., Varmeh, S., Kozma, S.C., Thomas, G., et al. (2010). A novel type of cellular senescence that can be enhanced in mouse models and human tumor xenografts to suppress prostate tumorigenesis. J Clin Invest *120*, 681-693.
38. Debnath, J., Muthuswamy, S.K., and Brugge, J.S. (2003). Morphogenesis and oncogenesis of MCF-10A mammary epithelial acini grown in three-dimensional basement membrane cultures. Methods *30*, 256-268.
39. Kotecha, N. (2010). Web based analysis and publication of flow cytometry experiments. Current Protocols in Cytometry *In press*.

Figure 1.

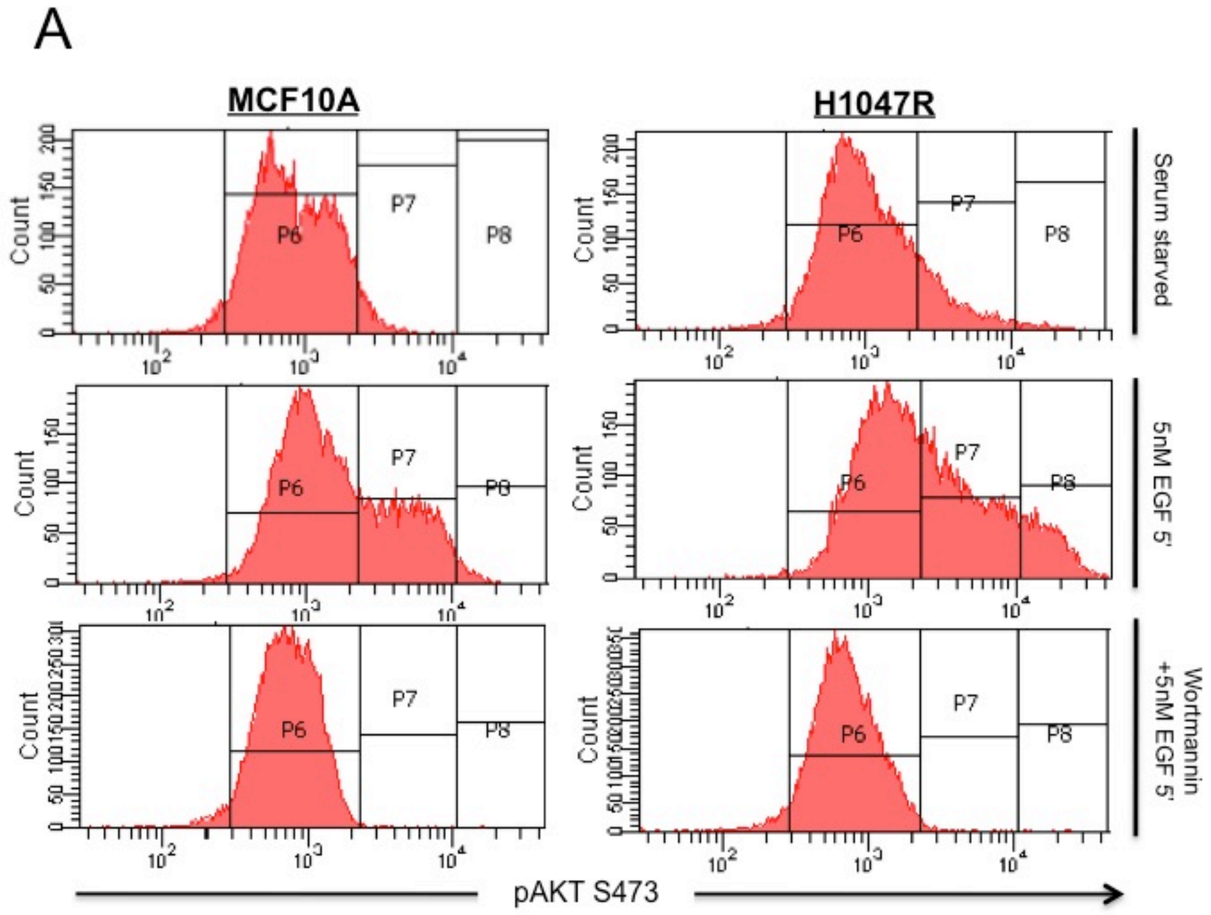
A
MCF10A
H1047R
Count
P6
P7
P8
Serum starved
5nM EGF 5'
Wortmannin +5nM EGF 5'
pAKT S473

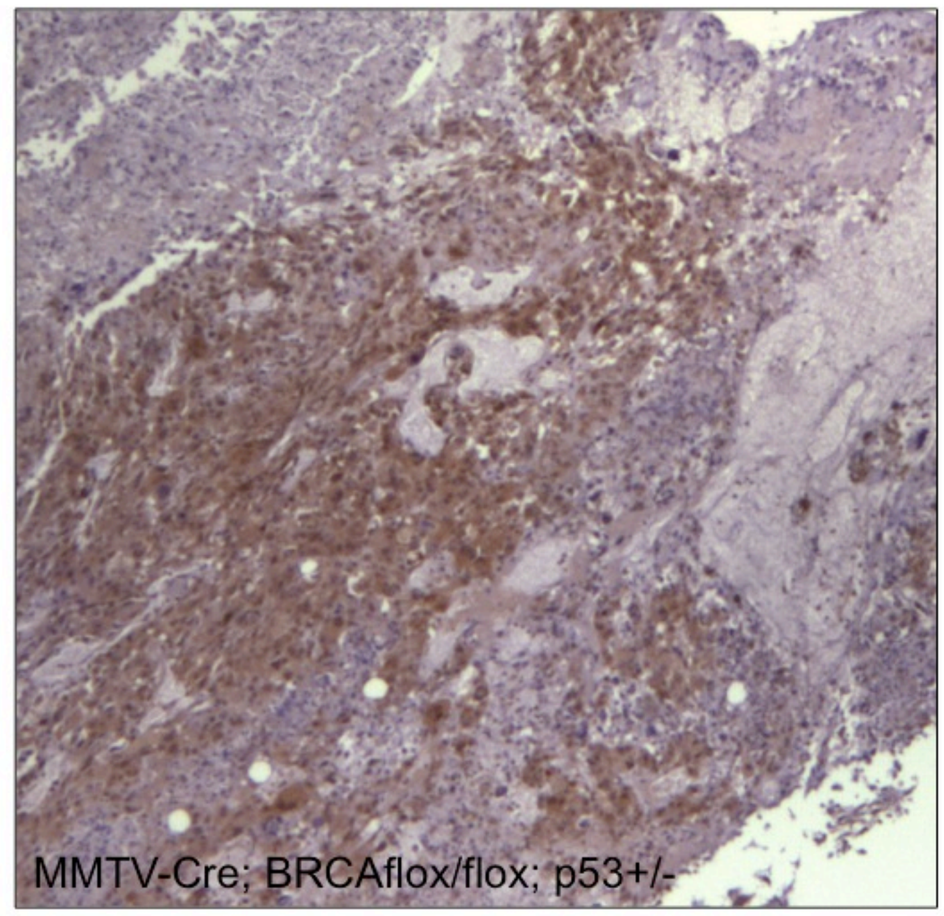
B
MMTV-Cre; BRCAflox/flox; p53+/-

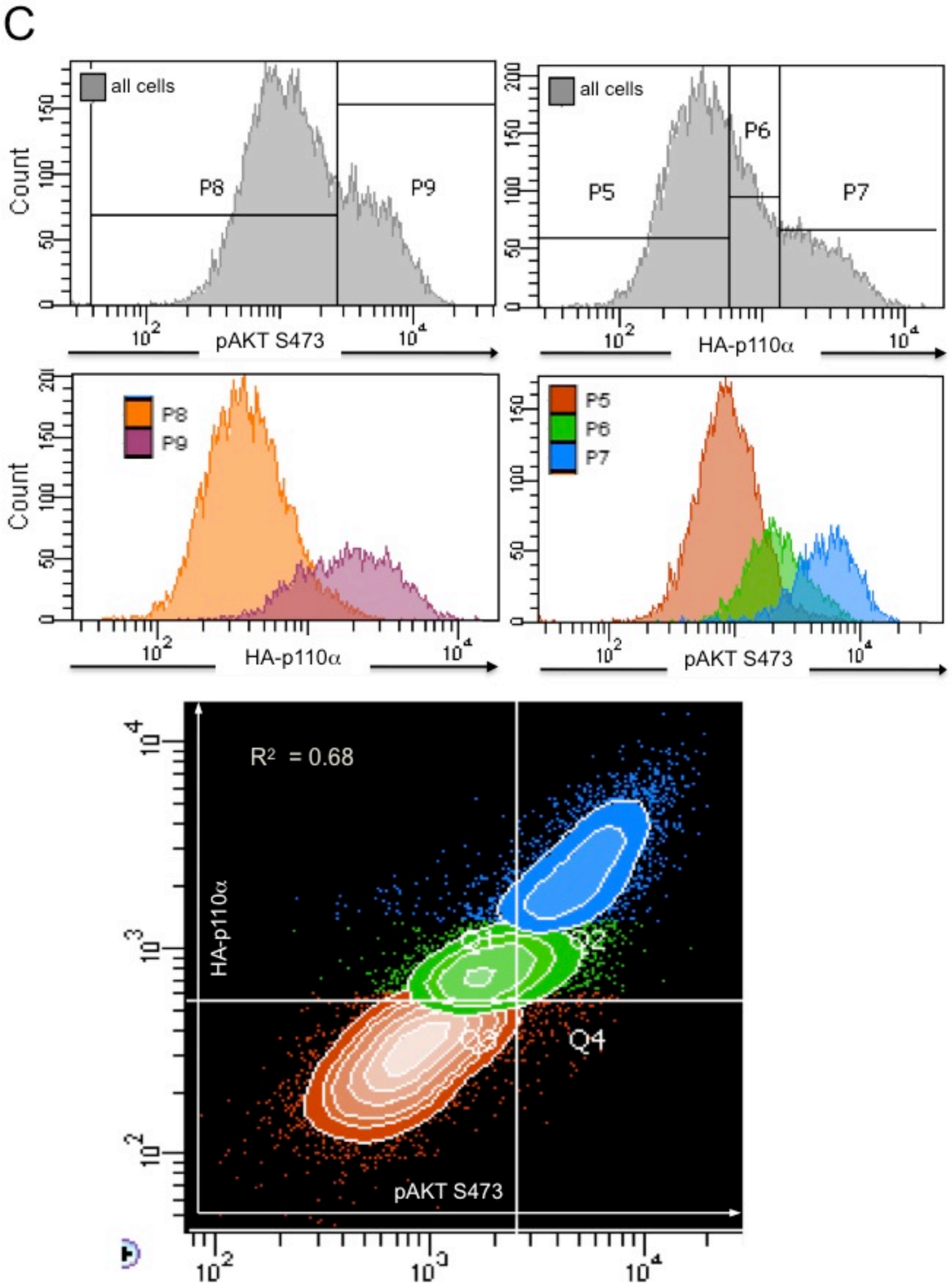
C
all cells
P8
P9
P5
P6
P7
Count
pAKT S473
HA-p110α
R² = 0.68
Q1
Q2
Q3
Q4

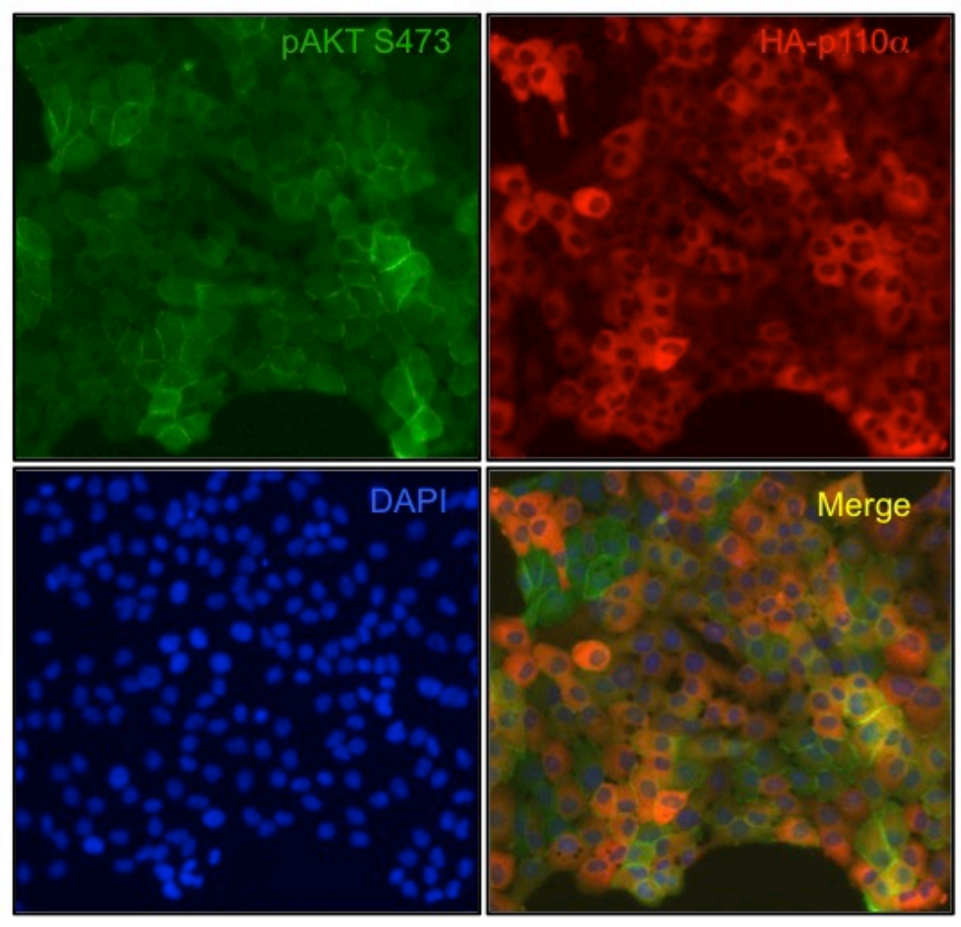
D
pAKT S473
HA-p110α
DAPI
Merge

Figure 2.

A

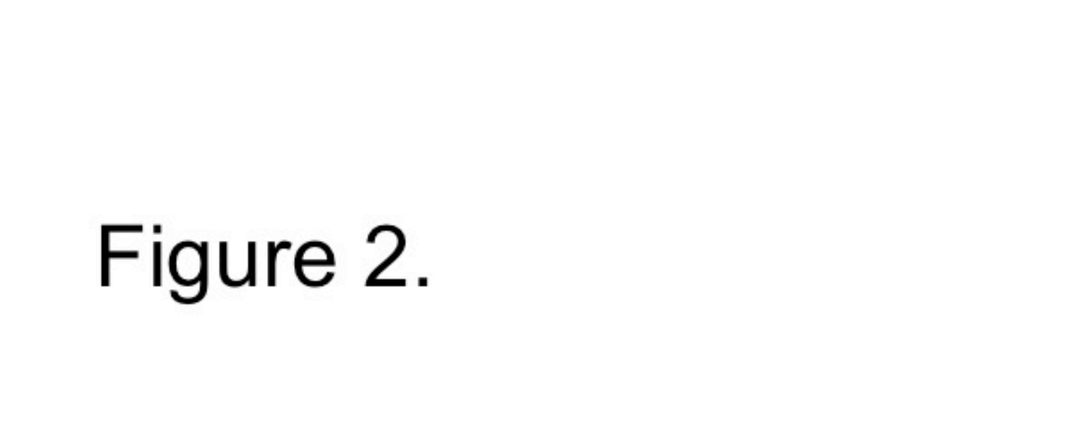

B

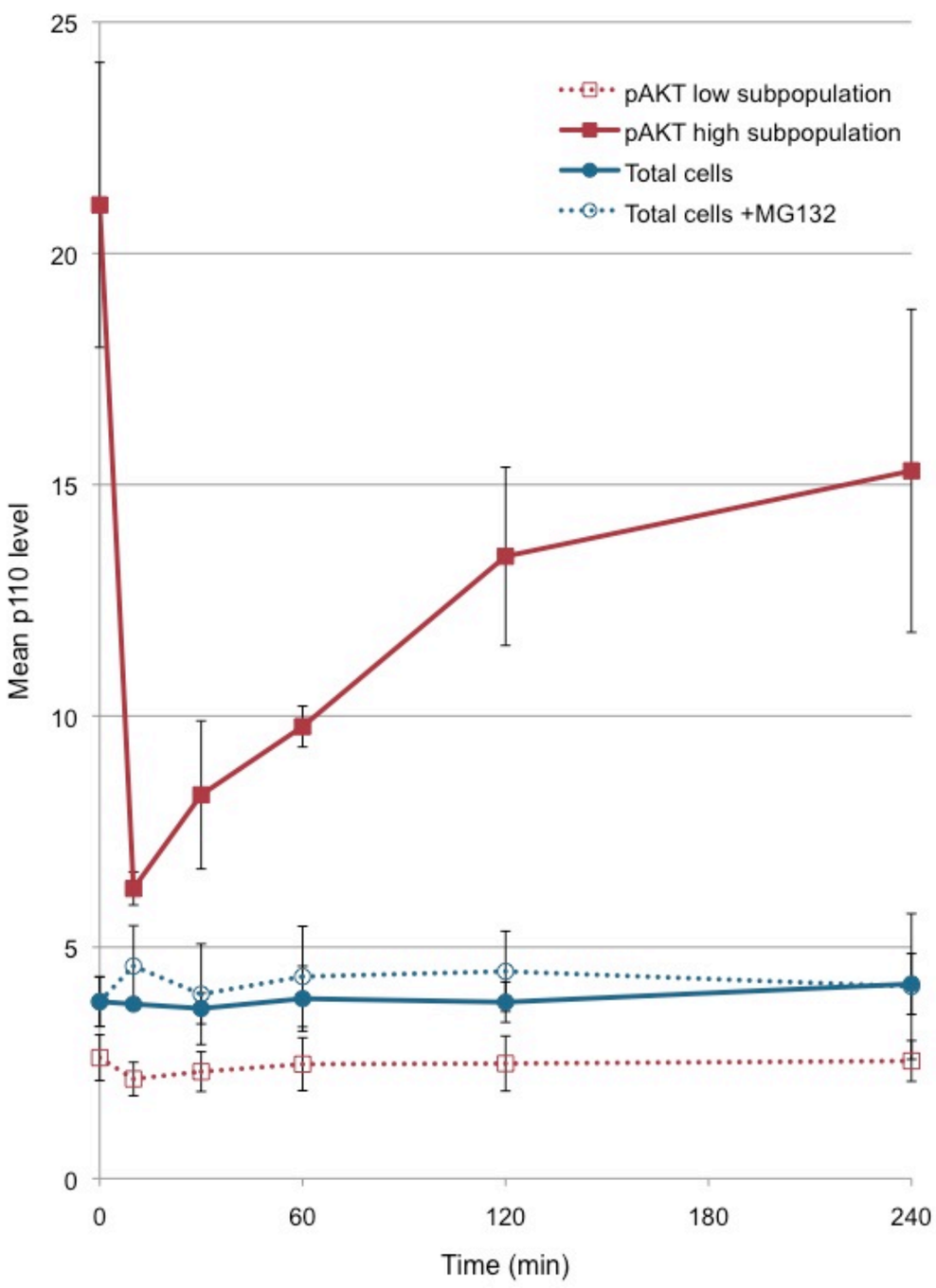

C

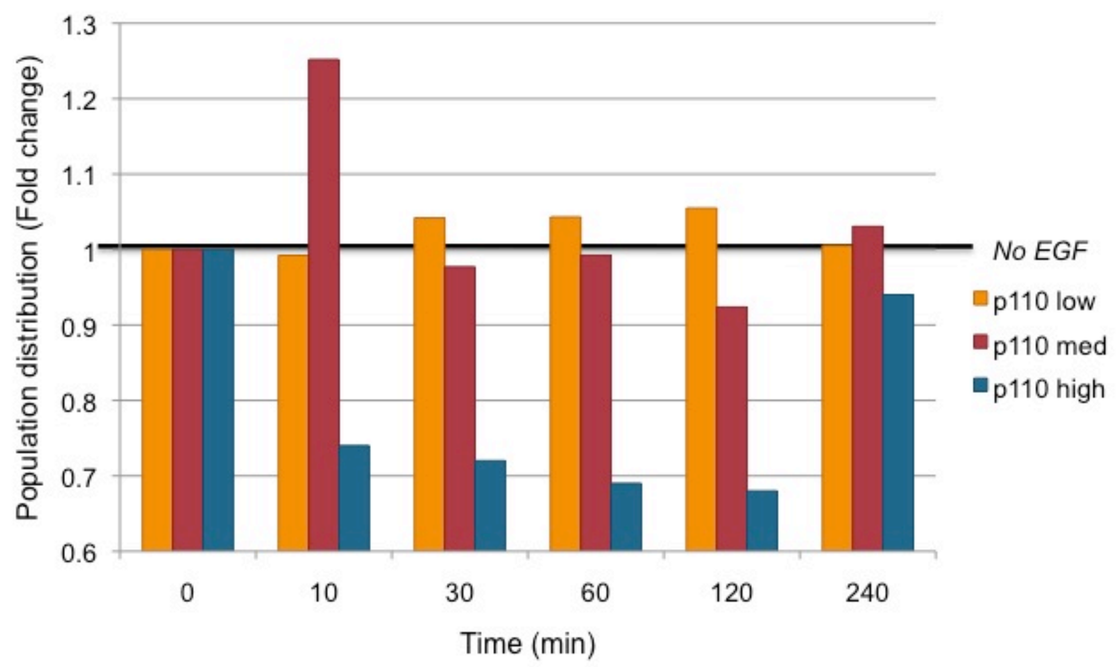

D

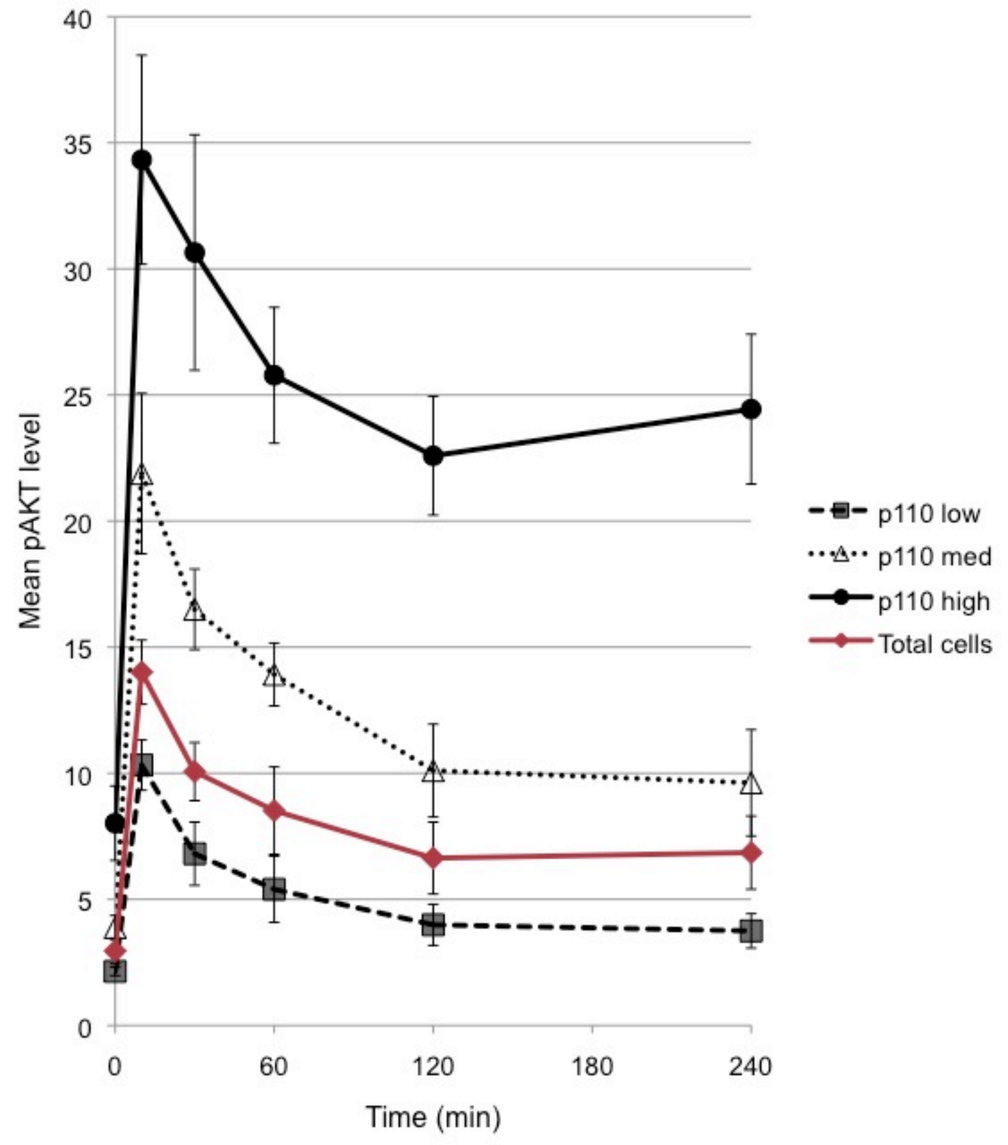

Figure 3.

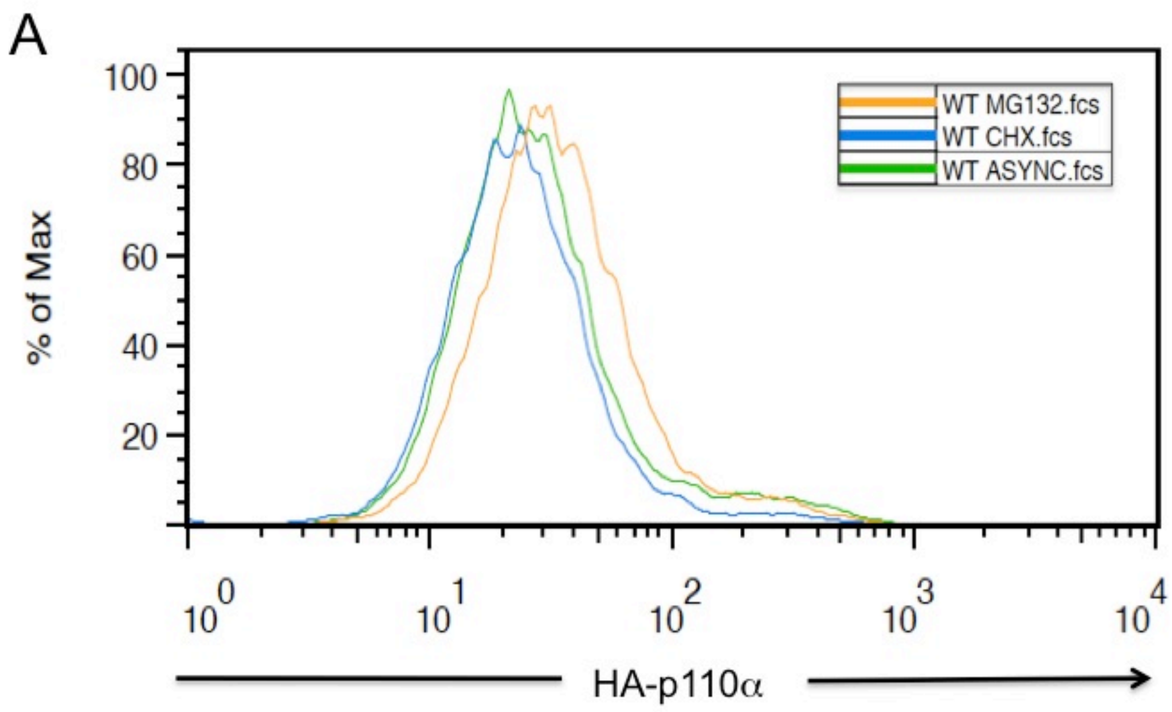
A
% of Max
HA-p110α
WT MG132.fcs
WT CHX.fcs
WT ASYNC.fcs

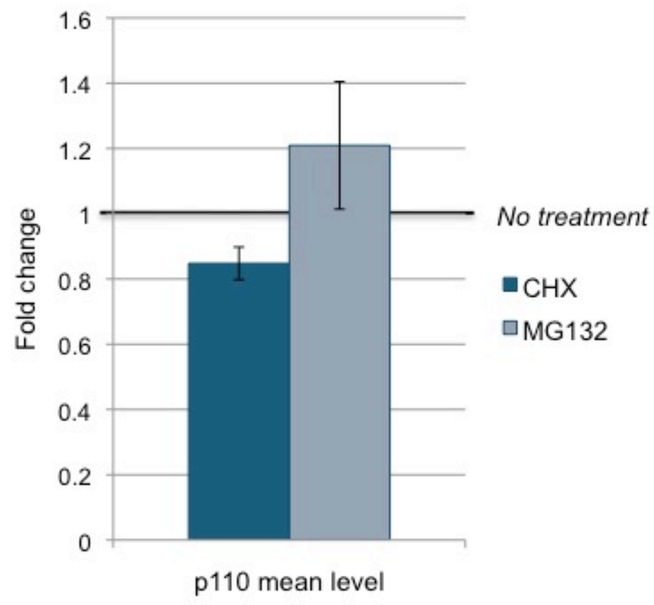
Fold change
No treatment
CHX
MG132
p110 mean level

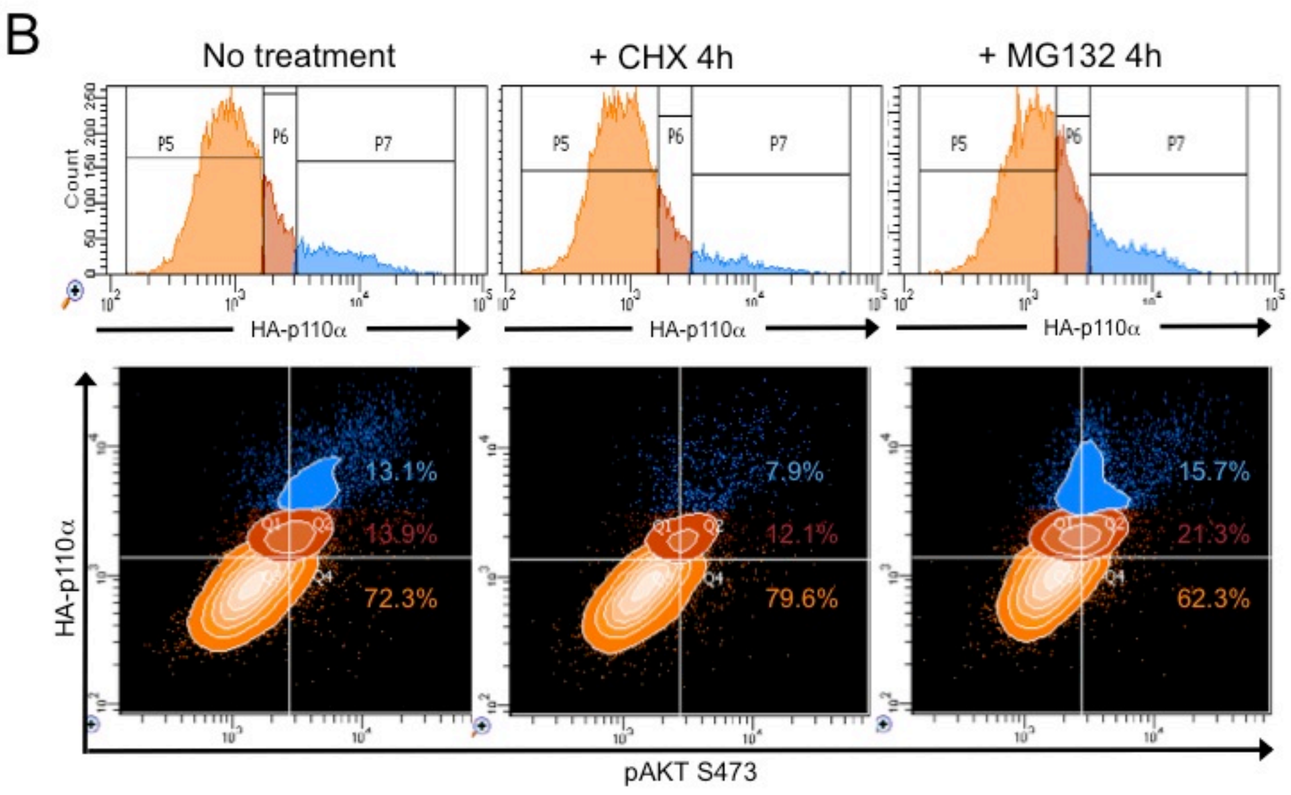
B
No treatment
+ CHX 4h
+ MG132 4h
P5
P6
P7
HA-p110α
13.1%
13.9%
72.3%
7.9%
12.1%
79.6%
15.7%
21.3%
62.3%
pAKT S473

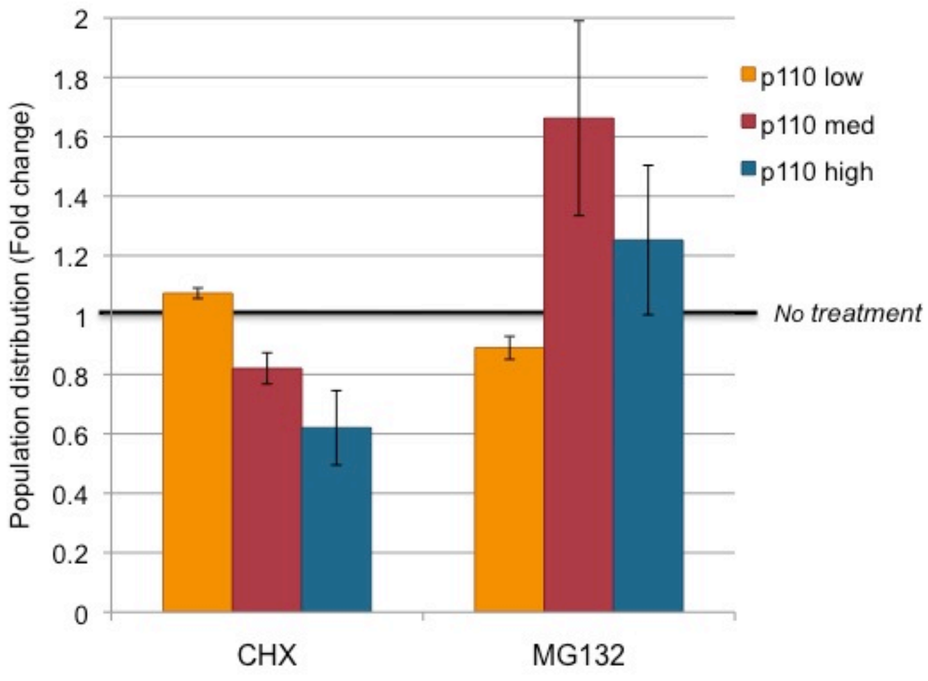
Population distribution (Fold change)
p110 low
p110 med
p110 high
No treatment
CHX
MG132

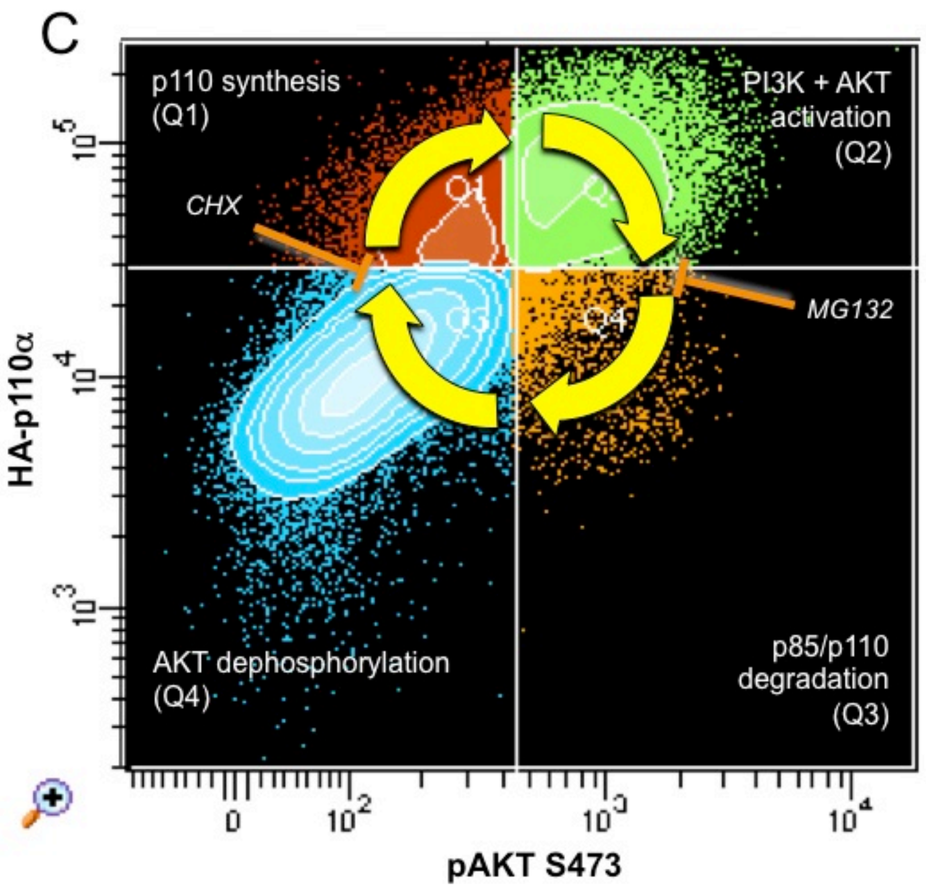
C
p110 synthesis
(Q1)
PI3K + AKT
activation
(Q2)
CHX
MG132
AKT dephosphorylation
(Q4)
p85/p110
degradation
(Q3)
HA-p110α
pAKT S473

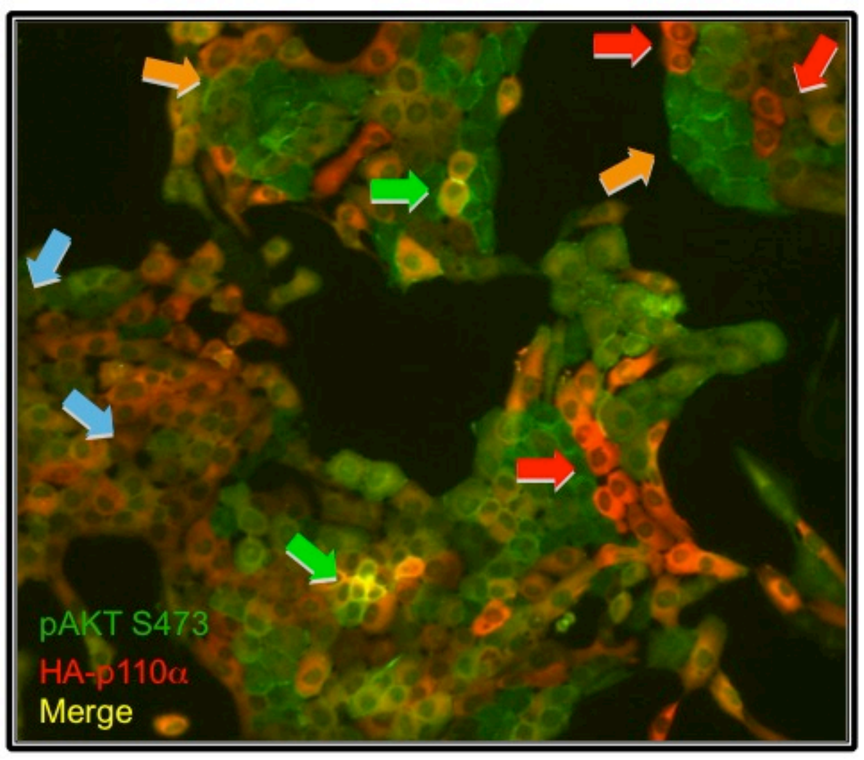
pAKT S473
HA-p110α
Merge

Figure 4.

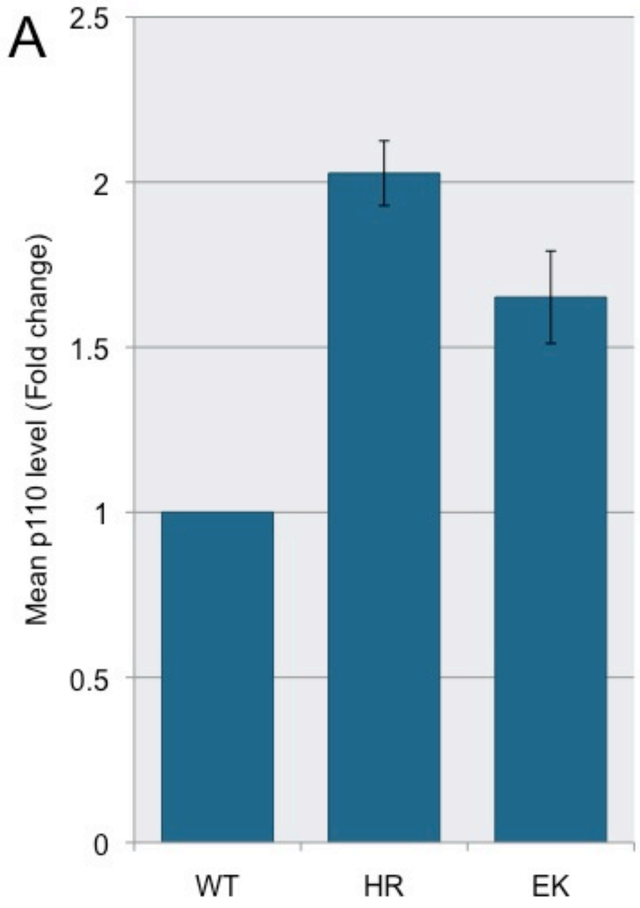
A
Mean p110 level (Fold change)
2.5
2
1.5
1
0.5
0
WT
HR
EK

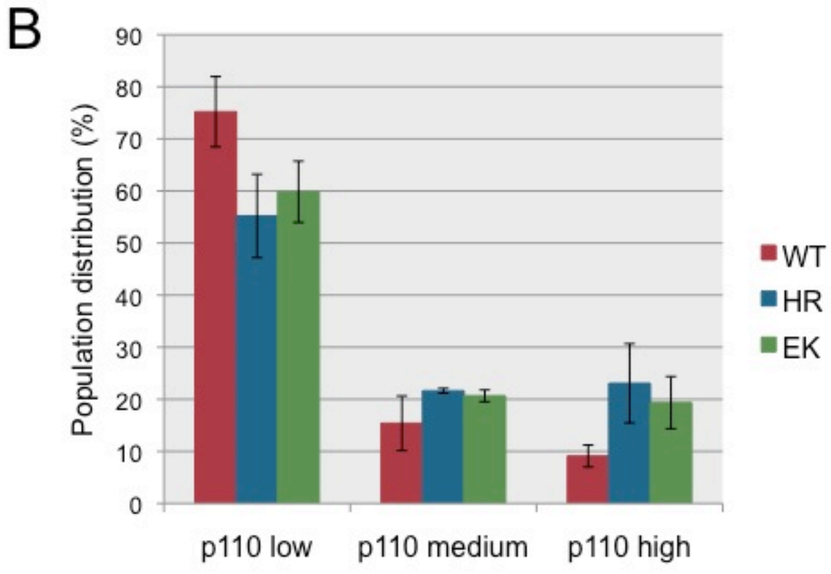
B
Population distribution (%)
90
80
70
60
50
40
30
20
10
0
p110 low
p110 medium
p110 high
WT
HR
EK

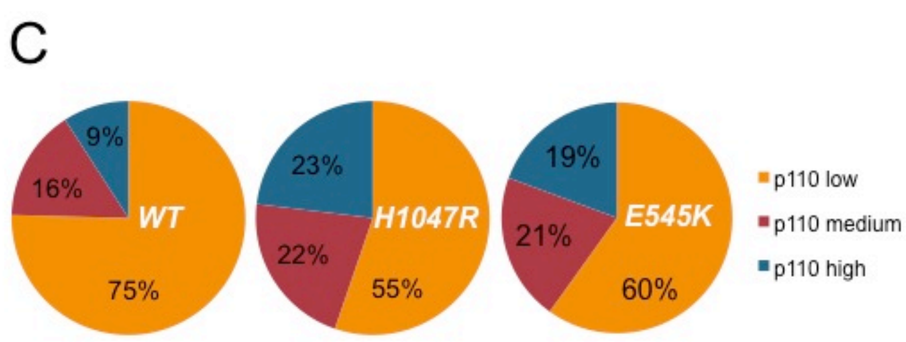
C
9%
16%
WT
75%
23%
H1047R
22%
55%
19%
21%
E545K
60%
p110 low
p110 medium
p110 high

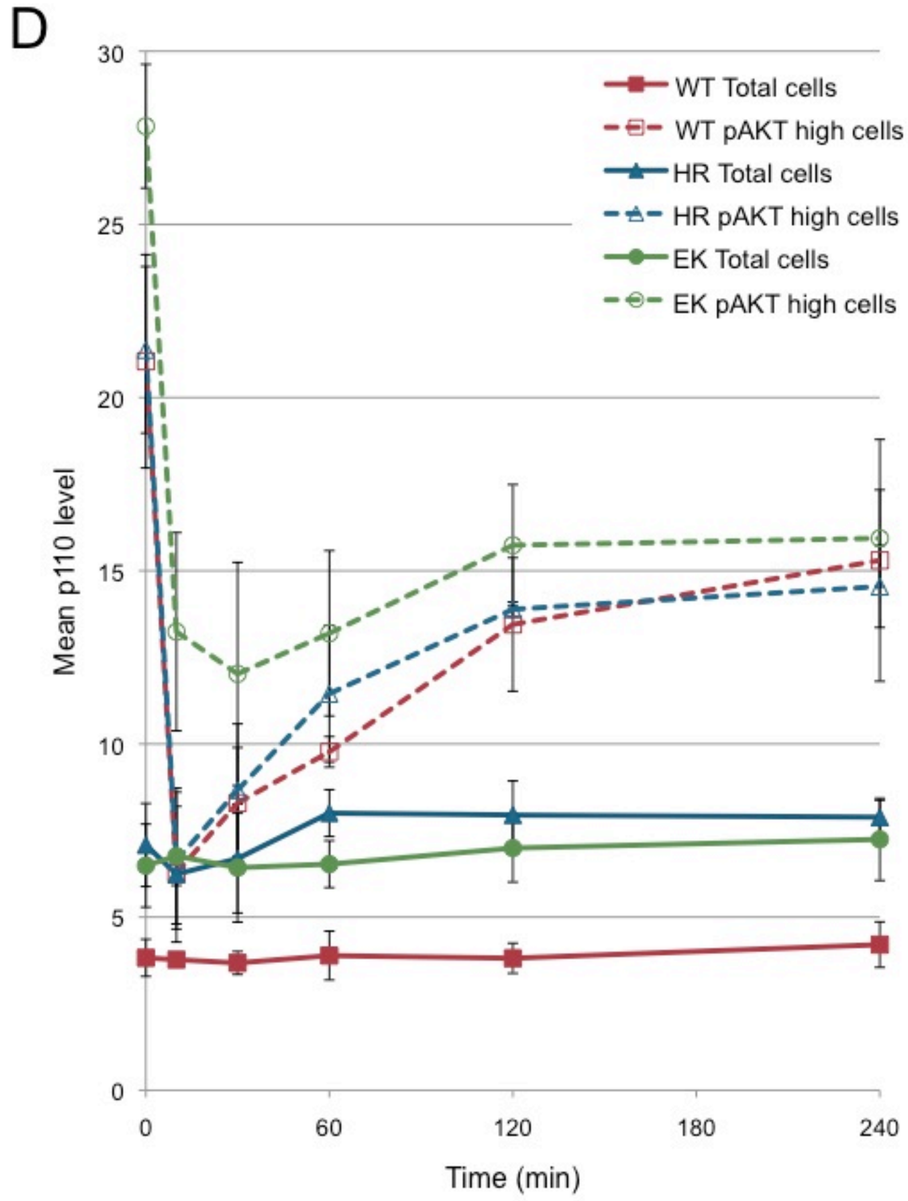
D
Mean p110 level
30
25
20
15
10
5
0
0
60
120
180
240
Time (min)
WT Total cells
WT pAKT high cells
HR Total cells
HR pAKT high cells
EK Total cells
EK pAKT high cells
*
*
*

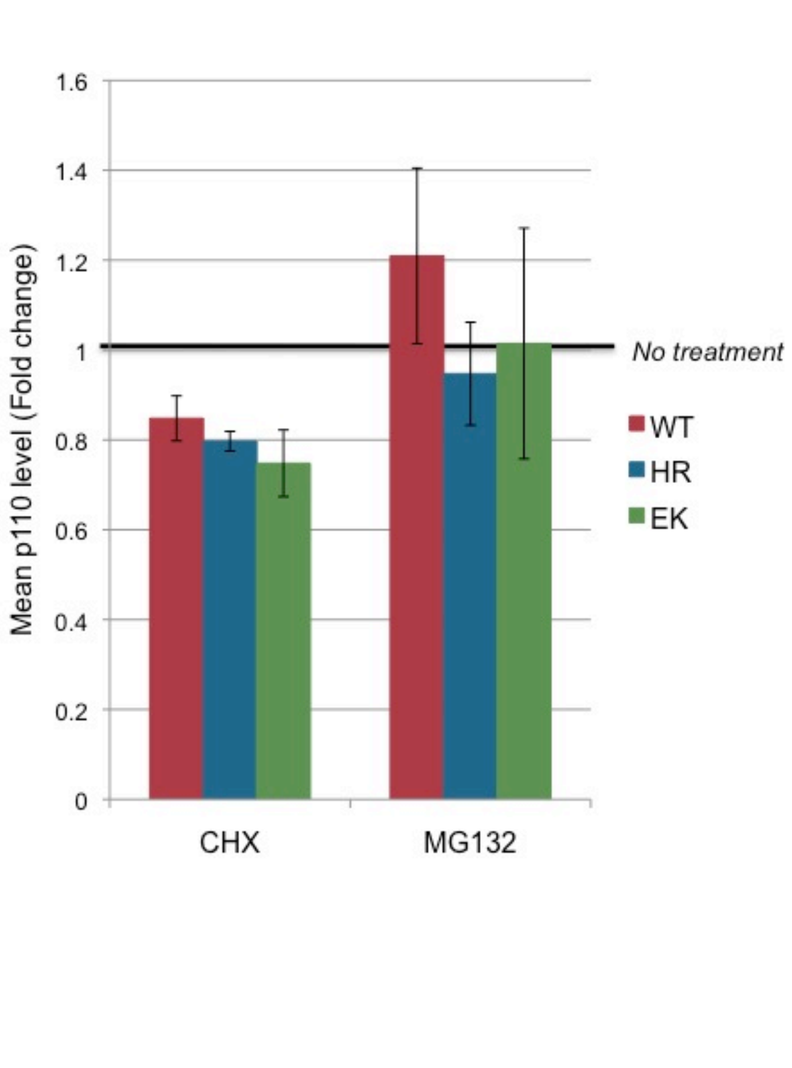
E
Mean p110 level (Fold change)
1.6
1.4
1.2
1
0.8
0.6
0.4
0.2
0
CHX
MG132
No treatment
WT
HR
EK

Figure 4.

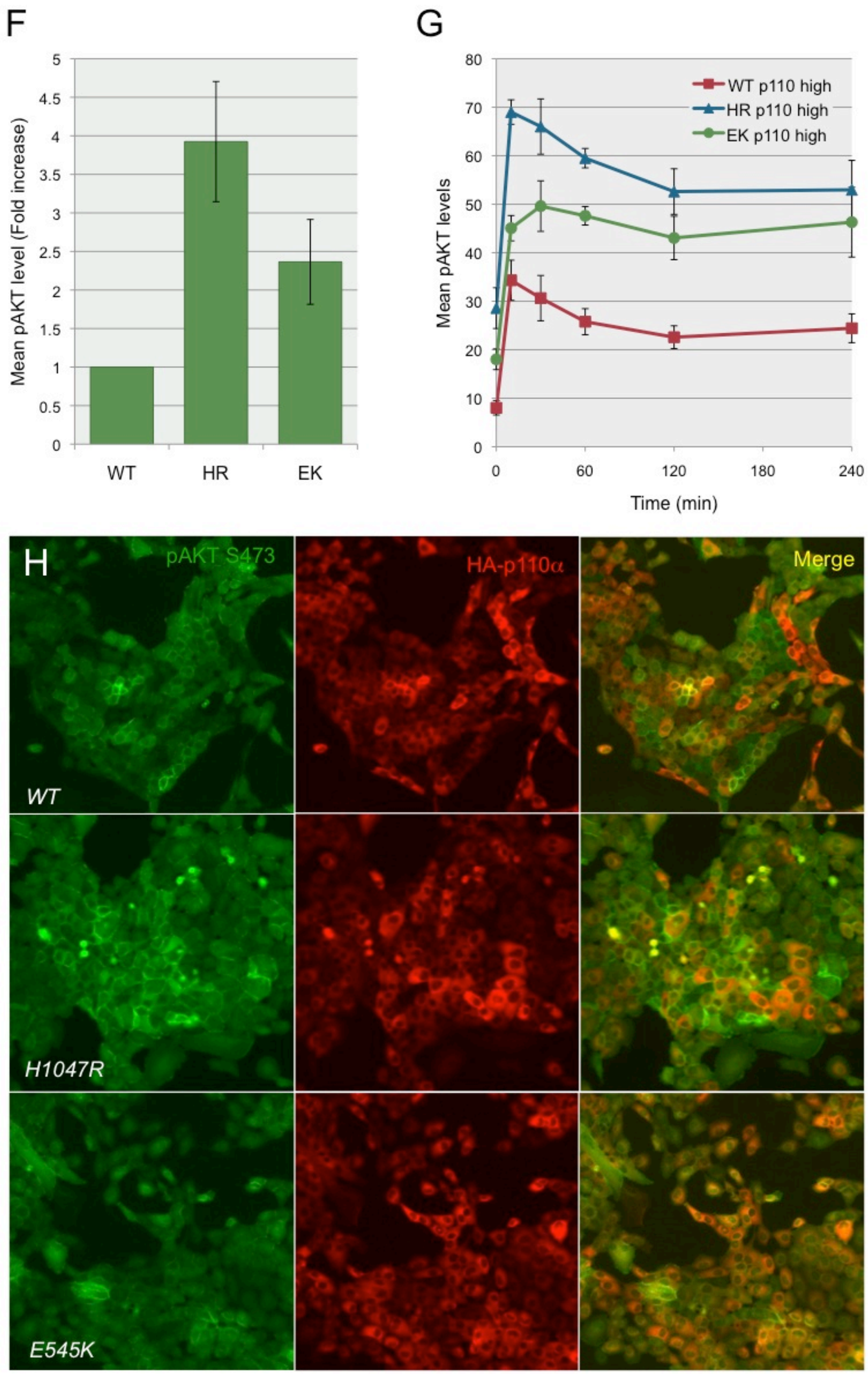
F
Mean pAKT level (Fold increase)
5
4.5
4
3.5
3
2.5
2
1.5
1
0.5
0
WT
HR
EK
G
Mean pAKT levels
80
70
60
50
40
30
20
10
0
0
60
120
180
240
Time (min)
WT p110 high
HR p110 high
EK p110 high
H
pAKT S473
HA-p110α
Merge
WT
H1047R
E545K

Figure 5.

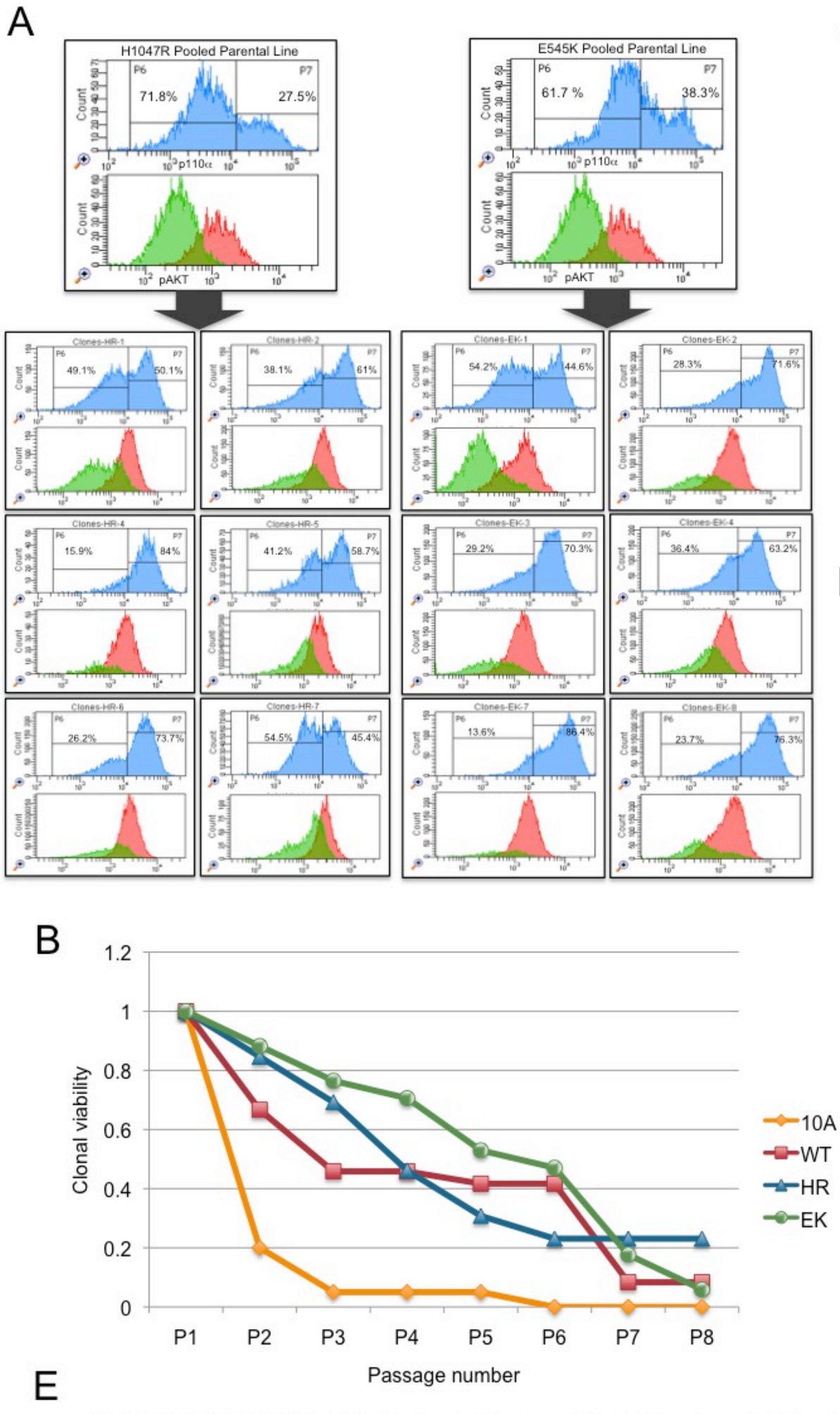
A
H1047R Pooled Parental Line
E545K Pooled Parental Line
P6
P7
71.8%
27.5%
61.7 %
38.3%
Count
p110α
pAKT
Clones-HR-1
49.1%
50.1%
Clones-HR-2
38.1%
61%
Clones-EK-1
54.2%
44.6%
Clones-EK-2
28.3%
71.6%
Clones-HR-4
15.9%
84%
Clones-HR-5
41.2%
58.7%
Clones-EK-3
29.2%
70.3%
Clones-EK-4
36.4%
63.2%
Clones-HR-6
26.2%
73.7%
Clones-HR-7
54.5%
45.4%
Clones-EK-7
13.6%
86.4%
Clones-EK-8
23.7%
76.3%
B
Clonal viability
Passage number
P1
P2
P3
P4
P5
P6
P7
P8
10A
WT
HR
EK
C
Early passage
Late passage
Clones-HR-1
Clonal reversion-HR-1
49.1%
50.1%
68.4%
28.4%
Clones-HR-2
Clonal reversion-HR-2
38.1%
61%
87.2%
11%
Clones-EK-3
Clonal reversion-EK-3
29.2%
70.3%
69%
29.8%
Clones-EK-8
Clonal reversion-EK-8
23.7%
76.3%
51.7%
47.8%
HA-p110α
D
% Cells with high p110α
WT-11
WT-3
WT-12
WT-15
WT-7
WT-2
WT-9
WT-6
WT-1
WT-8
WT-4
HR-5
HR-6
HR-7
HR-10
HR-1
HR-3
HR-8
HR-11
HR-9
EK-10
EK-8
EK-11
EK-14
EK-2
EK-15
EK-4
EK-9
EK-5
EK-7
EK-12
EK-3
EK-6
E
WT pool
Early passage
WT clone
Late passage
H1047R clone
Late passage
E545K clone
Late passage

Figure 6.

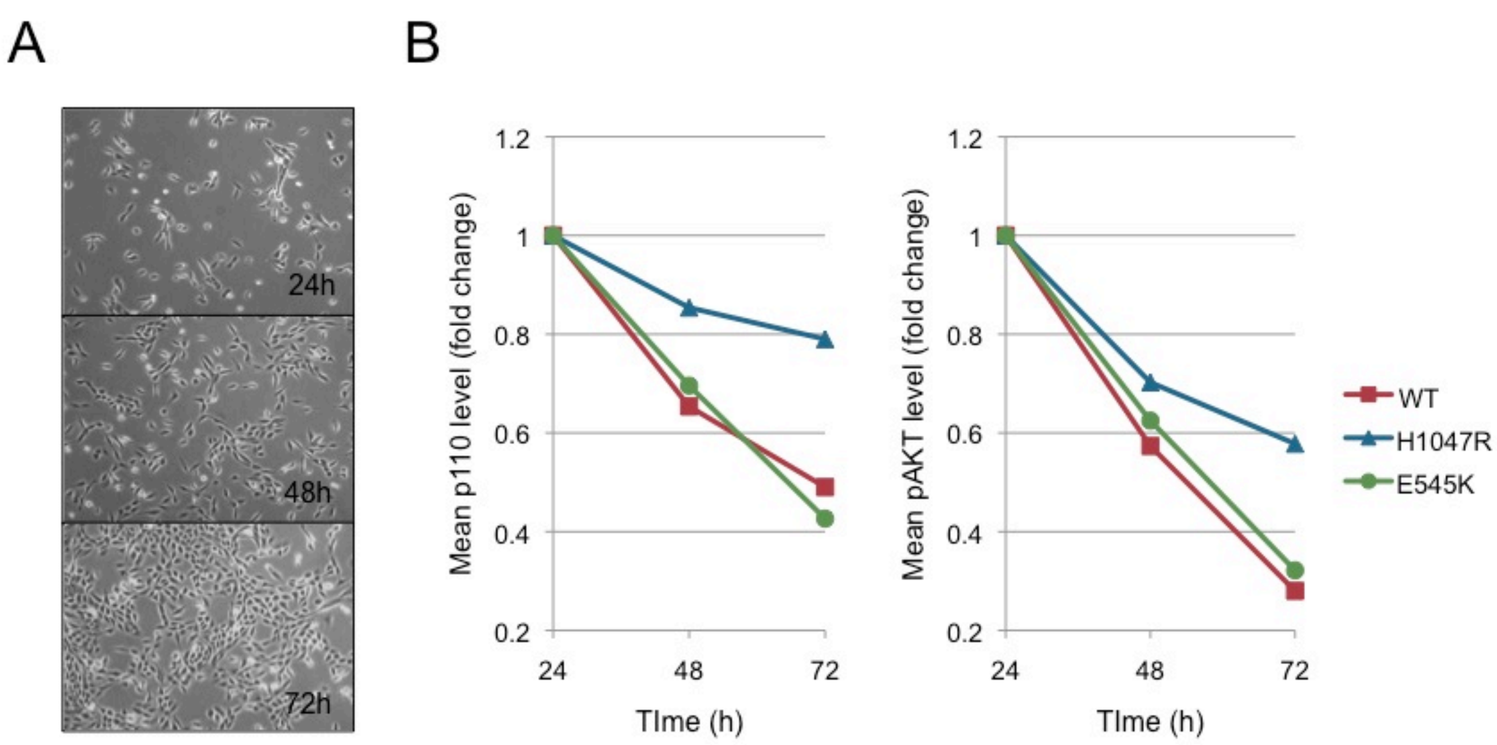
A
24h
48h
72h
B
Mean p110 level (fold change)
Mean pAKT level (fold change)
TIme (h)
WT
H1047R
E545K

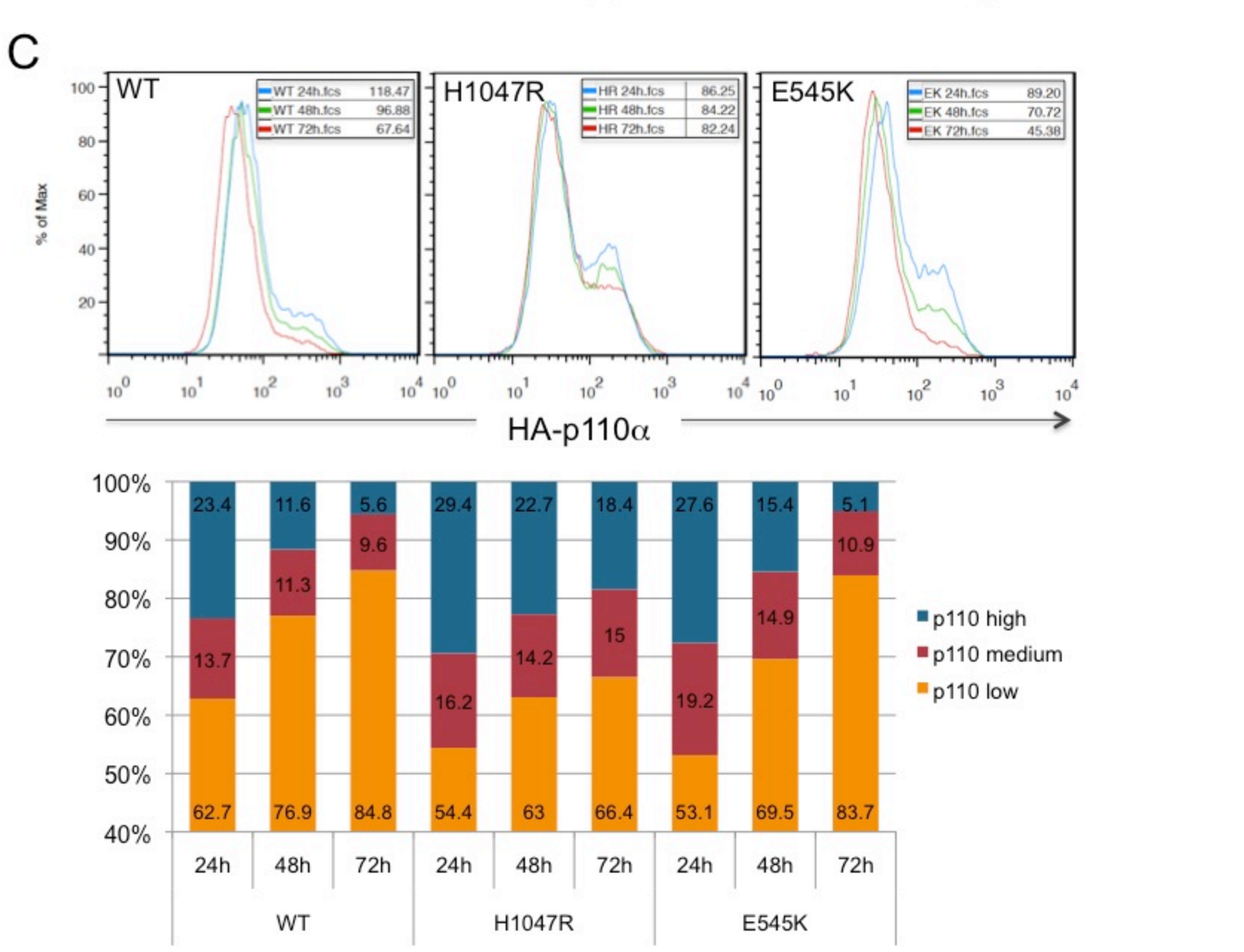
C
WT
H1047R
E545K
WT 24h.fcs 118.47
WT 48h.fcs 96.88
WT 72h.fcs 67.64
HR 24h.fcs 86.25
HR 48h.fcs 84.22
HR 72h.fcs 82.24
EK 24h.fcs 89.20
EK 48h.fcs 70.72
EK 72h.fcs 45.38
% of Max
HA-p110α
p110 high
p110 medium
p110 low
WT
H1047R
E545K

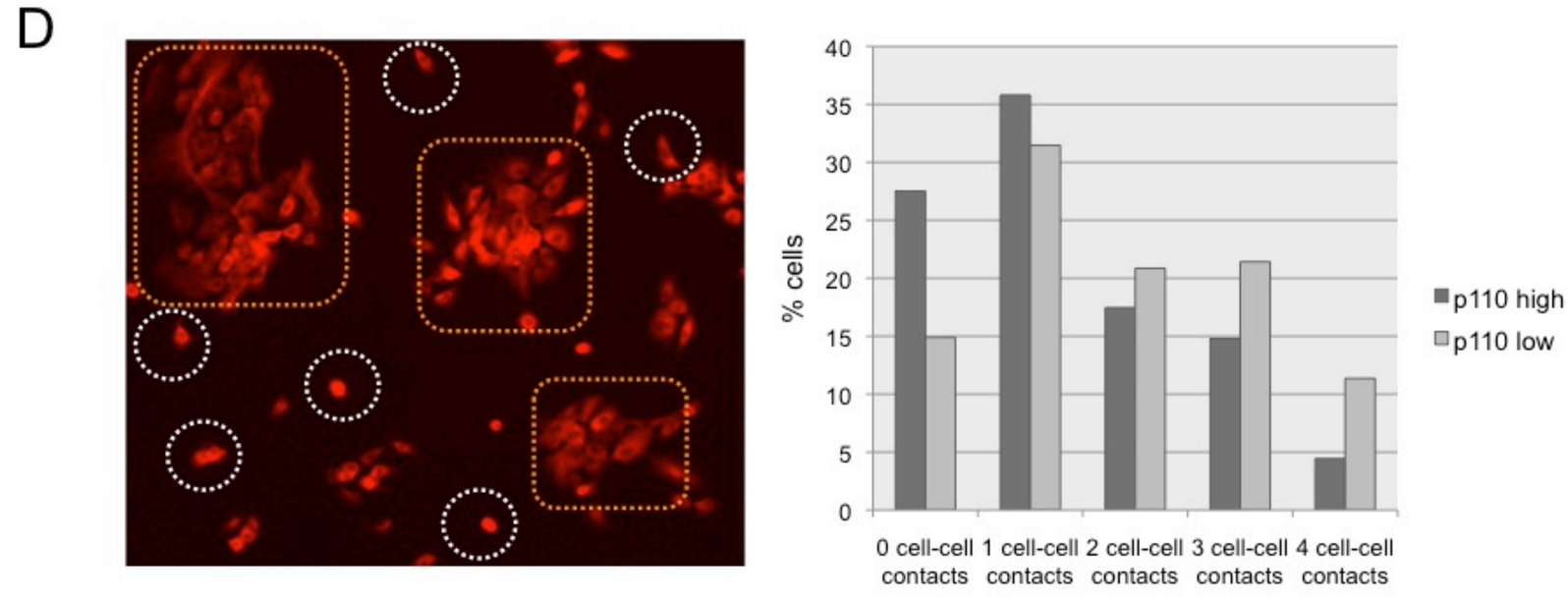
D
% cells
p110 high
p110 low
0 cell-cell contacts
1 cell-cell contacts
2 cell-cell contacts
3 cell-cell contacts
4 cell-cell contacts

Figure S1, related to Figure 1.

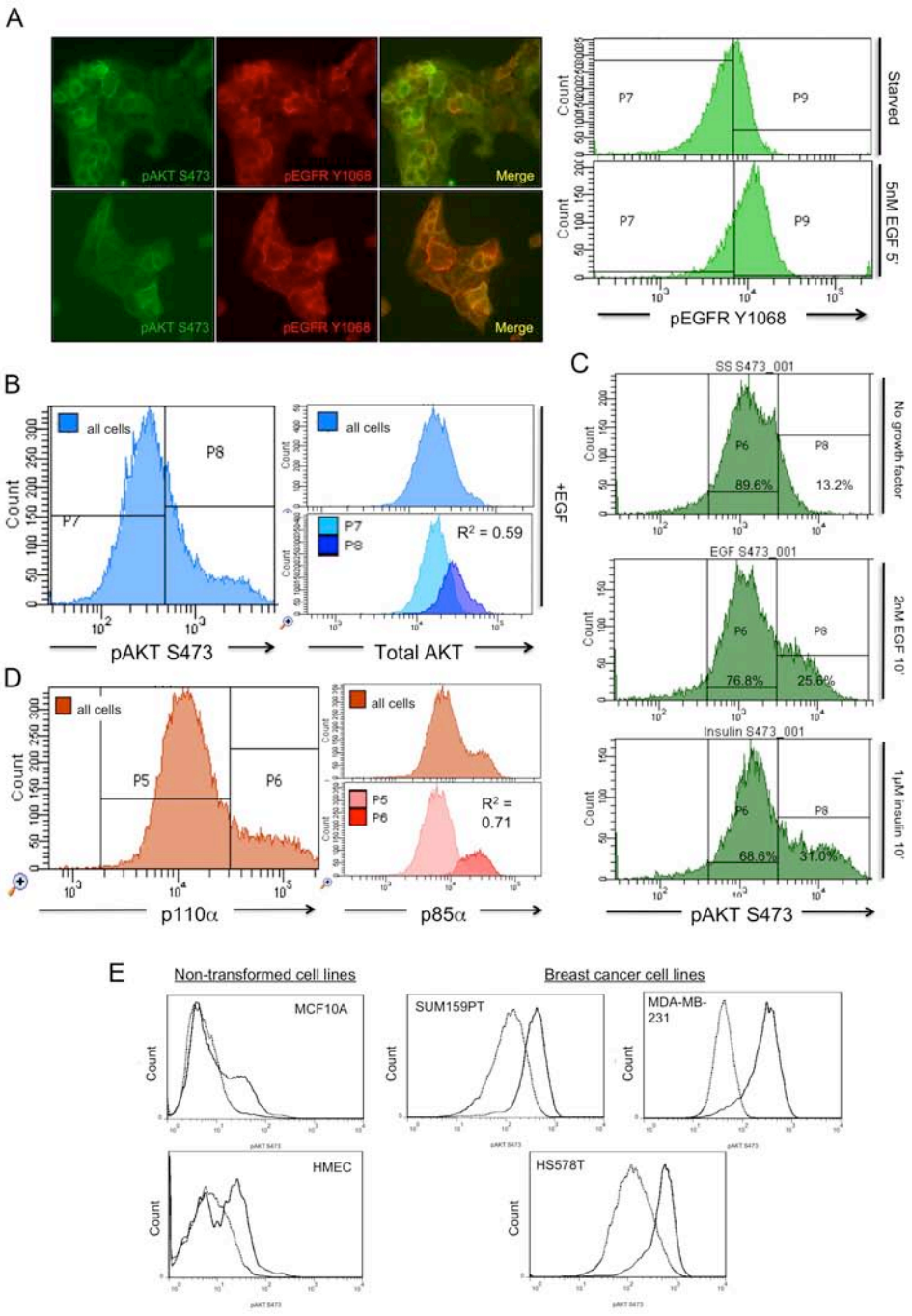

Figure S2, related to Figure 2.

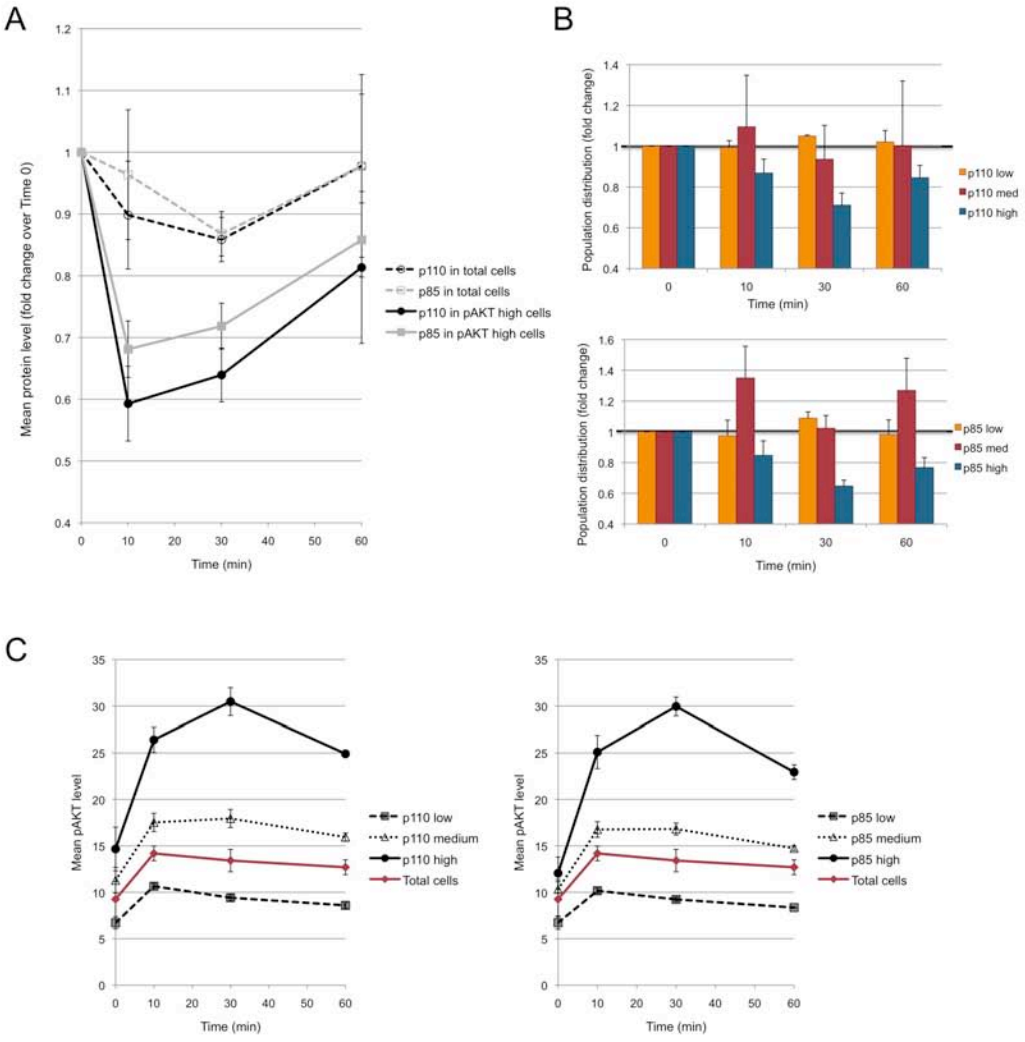

Figure S3, related to Figure 3.

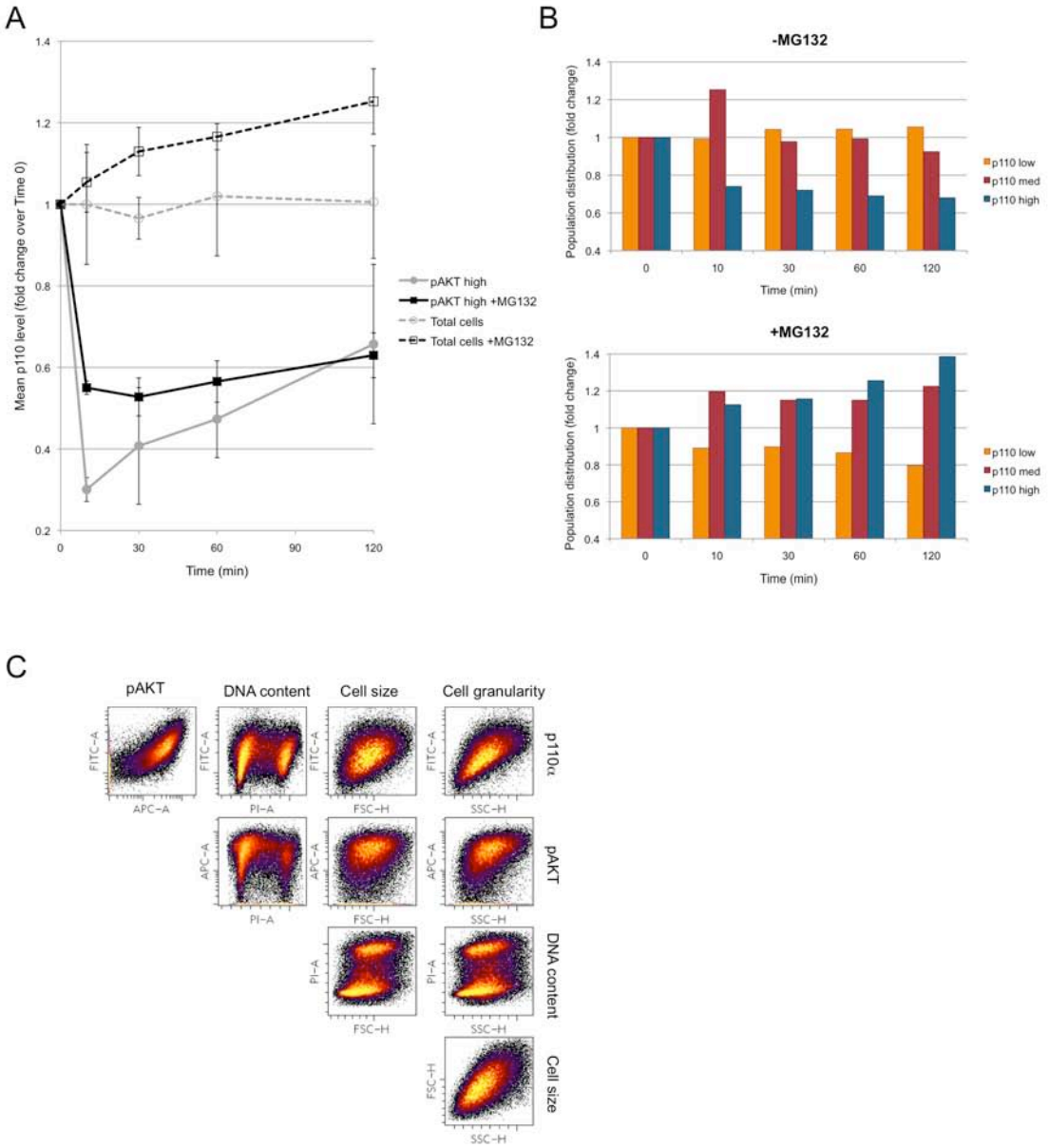

Figure S4, related to Figure 5

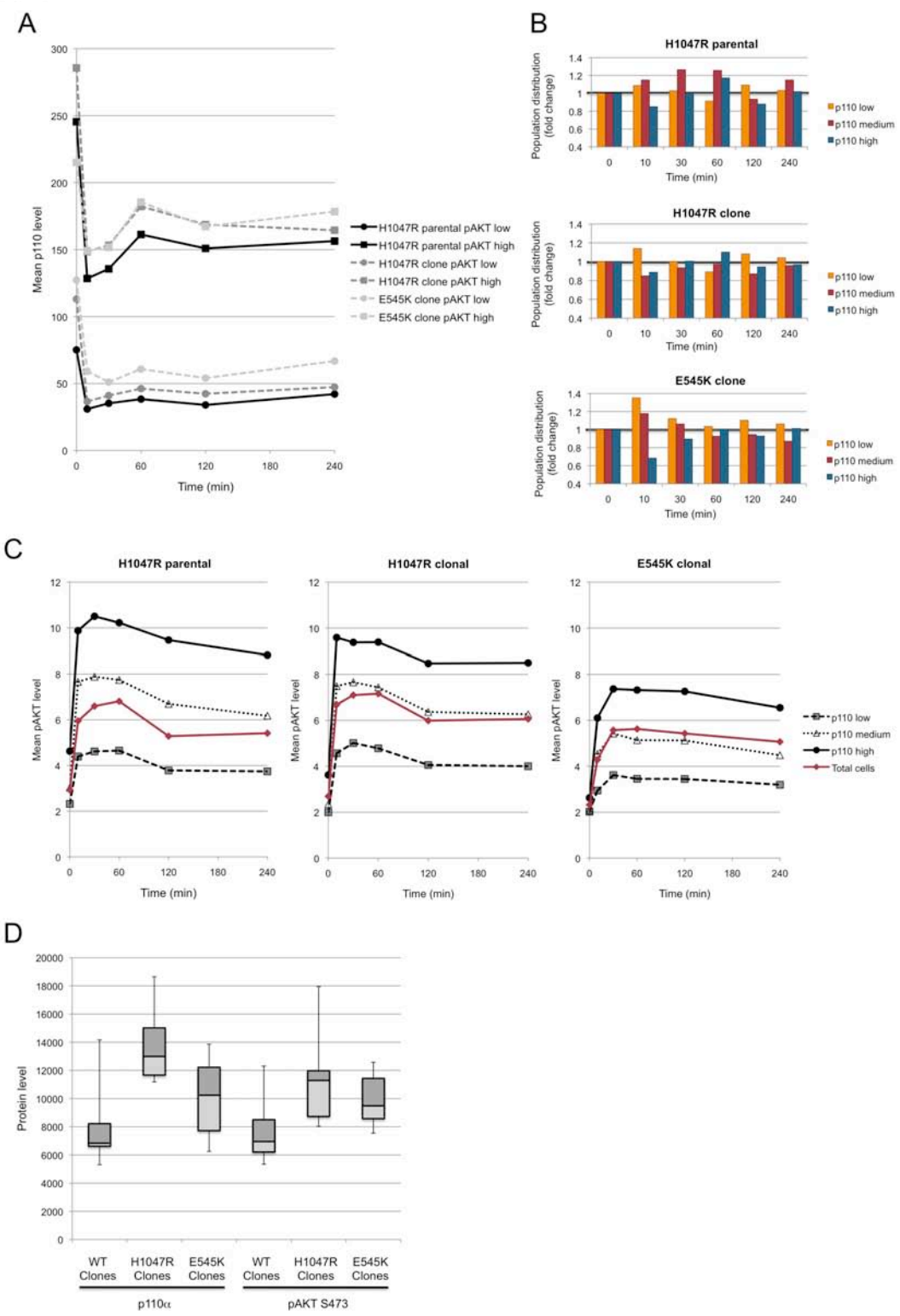

Figure S5, related to Figure 6.

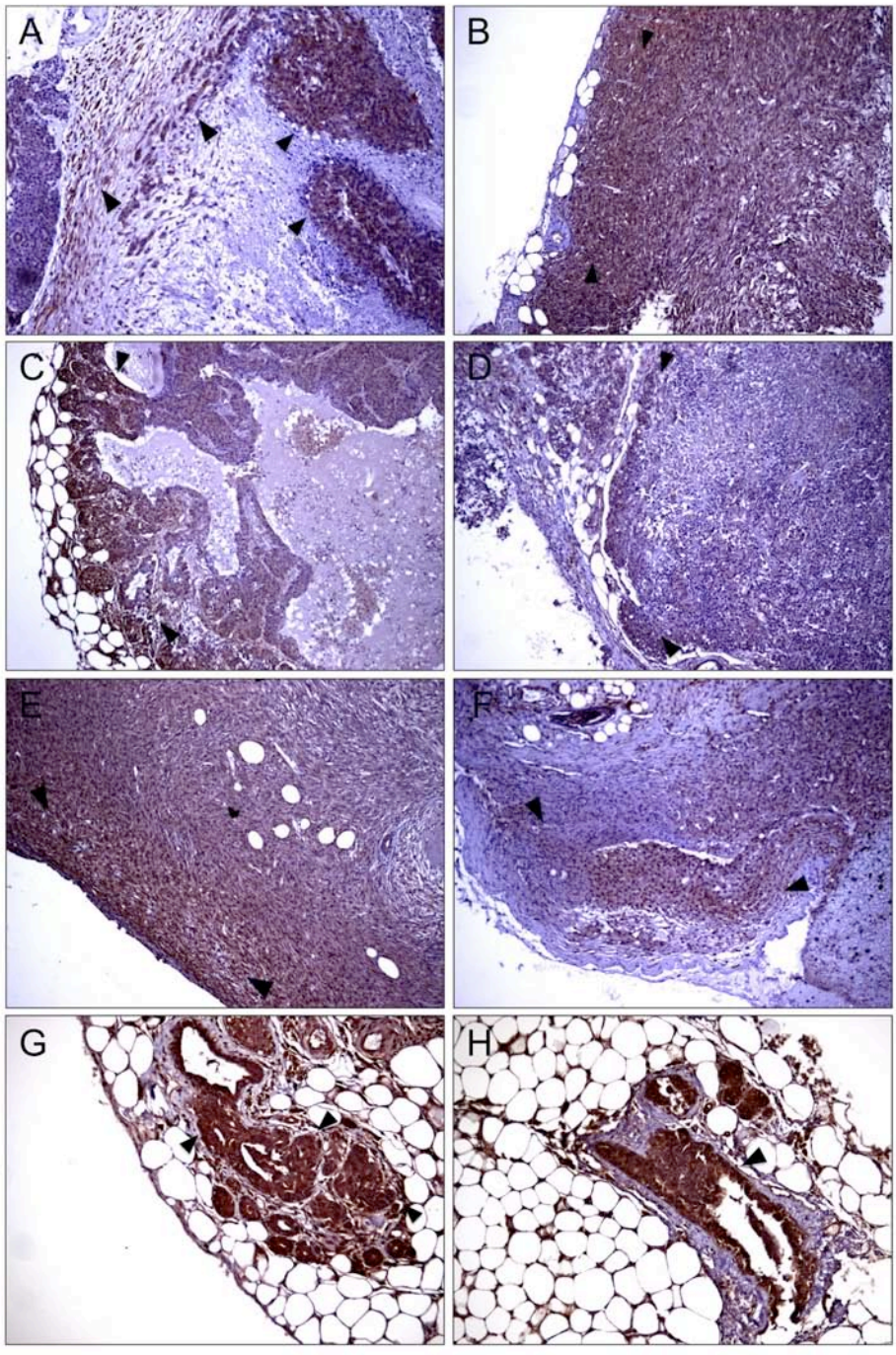

Figure S1, related to Figure 1. Correlation among other PI3K pathway members.

(A) EGFR activity does not correlate with AKT activity. MCF10A cells were serum and growth factor starved for 20h and acutely stimulated with 5nM EGF. (Left panels) Cells were fixed and co-stained with anti-pAKT S473 and pEGFR Y1068 antibodies and analyzed by immunofluorescence. Most cells display some degree of EGFR phosphorylation, however the amplitude of pEGFR staining does not correlate with pAKT status. (Right panels) Additionally, cells were stimulated with EGF, stained with anti-pEGFR Y1068 antibody, and analyzed by flow cytometry. EGF stimulated cells uniformly shift with a log-normal distribution to the positive gate (P9), in contrast to the bimodal distribution observed for pAKT S473.

(B) Total AKT level does not determine AKT activity. MCF10A cells were treated as described in (A). Cells were harvested and co-stained with anti-pAKT S473 and anti-total AKT antibodies and analyzed by flow cytometry. (Top right panel) Total AKT levels are log-normal in MCF10A populations, compared to pAKT S473 levels (left panel), which are bimodal. pAKT-positive cells (P8) have slightly higher levels of total AKT than pAKT-negative cells (P7), however there is significant overlap between the two populations, weakening the correlation (R^2=0.59).

(C) Bimodal AKT activation is not ligand-specific. MCF10A cells were serum and growth factor starved and acutely stimulated with 2nM EGF or 1μM insulin for 10 minutes. Cells were harvested and stained for pAKT S473 and analyzed by flow cytometry. Similar bimodal distributions of AKT activity were obtained with EGF and insulin stimulation, suggesting that heterogeneous AKT activation is not a ligand-specific effect.

(D) p85α level correlates with p110α level. MCF10A cells expressing HA-p110α were harvested and co-stained with anti-HA and anti-p85α antibodies. (Top right panel) Endogenous p85α levels segregate into a bimodal distribution, similar to HA-p110α levels (left panel). $p110\alpha^{high}$ cells (P6) are also $p85\alpha^{high}$ and $p110\alpha^{low}$ cells (P5) are $p85\alpha^{low}$, conferring a strong correlation (R^2=0.71).

(E) Two non-transformed mammary epithelial cell lines, MCF10A and HMEC, and three transformed breast cancer cell lines, SUM159PT, HS578T and MDA-MB-231, were serum starved for 24 hours and acutely stimulated with saturating doses of growth factors (5nM EGF + 1uM insulin) for 10 minutes to maximally activate endogenous PI3K within the cell population. Cells were harvested as described in the Methods and analyzed by flow cytometry for phosphorylation of AKT at S473. Dotted lines represent AKT activity in starved cells and solid lines represent AKT activity in stimulated cells. Only non-transformed cells exhibited distinct bimodality, while the transformed cells exhibited a more complete shift to AKT positivity. This suggests that in non-transformed cells AKT activity is negatively regulated, perhaps via the modulation of PI3K protein levels as described in this manuscript. In order to achieve oncogenic levels of AKT activity, cancer cells may override this negative regulation by maintaining constitutively high levels of PI3K or perhaps by some means of lowering the threshold for PI3K-AKT activation.

Figure S2, related to Figure 2. p85α kinetics closely mirror p110α kinetics during a timecourse of EGF stimulation.

(A) MCF10A cells were serum starved and stimulated with 5nM EGF. p85α and HA-p110α protein levels were measured at various time points by flow cytometry using antibodies against endogenous p85α and HA. As shown in Figure 2A, HA-p110α levels in the

pAKT-high population drop precipitously at 10 minutes. This drop is mirrored by endogenous p85α levels, which drop to a similar but slightly lesser degree. This may be explained by the fact that there is more p85α than p110α in the cell, and monomeric p85α may not be subject to the same degradation mechanism as heterodimerized p85α.

(B) The distribution of cells within the $p85\alpha^{low}$, $p85\alpha^{medium}$ and $p85\alpha^{high}$ populations closely resembles the distribution within p110α populations, including the drop in the proportion of $p85\alpha^{high}$ cells at 10 minutes, which correlates with the drop in p85α protein levels in (A).

(C) The AKT activity of cells within the $p85\alpha^{low}$, $p85\alpha^{medium}$ and $p85\alpha^{high}$ populations closely resembles those of p110α populations, with the $p85\alpha^{high}$ population driving maximal AKT activity within the total population.

Figure S3, related to Figure 3. MG132 treatment can stabilize p110α levels during EGF stimulation.

(A) Cells were serum starved for 24 hours and pre-treated with 50uM MG132 for 1h prior to 5nM EGF stimulation. p110α levels were measured at various time points by flow cytometry. MG132 treatment resulted in a partial rescue of p110α degradation at 10 minutes and an overall increase in p110α protein in the total cell population. We were unable to achieve a complete rescue of p110α degradation, which may be due to the fact that we were unable to treat cells with higher concentrations of MG132 or for longer durations without greatly altering AKT activity. It is also possible that p110 degradation is carried out by cellular proteases in addition to the proteosome.

(B) 50uM MG132 treatment was also sufficient to block the drop in the proportion of cells in the p110α^{high} state at 10 minutes that is observed in untreated cells.

(C) The raw data from the 24h timepoint in the experiment described in Table S1 are plotted as dot plots to demonstrate little to no correlation between any parameter parings besides pAKT and p110α protein.

Figure S4, related to Figure 5. Late passage clonal cell lines behave similarly to parental pooled cell lines after reversion to the parental bimodal distribution.

(A) Two late passage clonal cell lines and one parental cell line were serum starved for 24 hours and acutely stimulated with 5nM EGF. p110α levels were measured at various time points by flow cytometry. Despite having the reversed bimodal profile at early passage, late passage clonal cell lines that have reverted to the parental distribution exhibit the same p110α kinetics as parental cell lines.

(B) Population distributions in late stage clonal cell lines resemble the population distribution of a parental cell line, including the drop in the proportion of cells in the p110α^{high} state at 10 minutes.

(C) In clonal cell lines, the AKT activity of cells within the p110α^{low}, p110α^{medium} and p110α^{high} populations closely resembles those of a parental cell line, with the p110α^{high} population driving maximal AKT activity within the total population.

(D) Clonal cell lines derived from WT, H1047R or E545K parental pooled cell lines were harvested at intermediate passages and analyzed for p110α levels and AKT activity

following serum starvation and acute 5nM EGF stimulation. As we showed for parental cell lines in Figure 4A, clonal cells lines expressing mutant *PIK3CA* have higher levels of p110α and pAKT than clonal cell lines expressing wildtype *PIK3CA.*

Figure S5, related to Figure 6. pAKT is enriched at pushing margins and ductal hyperplasias.

(A) Mammary tumors from MMTV-Cre; BRCA1 flox;flox; p53+/- mice were stained for pAKT S473. Near the center of the tumor, pAKT-positive cells are heterogeneously distributed, as indicated by arrowheads.

(B-F) pAKT is enriched at the non-invasive, smooth edges of these tumors, referred to as "pushing margins". Arrowheads roughly enclose these margins in five separate MMTV-Cre; BRCA1 flox;flox; p53+/- tumors.

(G-H) pAKT is also enriched in the lumens of ductal hyperplasias (arrowheads).

Table S1, related to Figure 3.

	R-squared value			
Parameter pairing	24h	48h	72h	96h
p110, pAKT	**0.523**	**0.536**	**0.596**	**0.447**
p110, DNA content	0.017	0.004	0.003	0.006
p110, Cell size	0.030	0.156	0.155	0.171
p110, Cell granularity	0.332	0.277	0.280	0.330
pAKT, DNA content	0.033	0.091	0.125	0.260
pAKT, Cell size	0.144	0.046	0.038	0.005
pAKT, Cell granularity	0.262	0.193	0.220	0.209
DNA content, Cell size	0.127	0.172	0.194	0.206
DNA content, Cell granularity	0.044	0.046	0.032	0.026
Cell size, Cell granularity	0.357	0.384	0.369	0.350

Table S2, related to Figure 5.

Parental Population	Colonies formed	Survival to P2	P4 Clones with high p110α
MCF10A	20/48 (0.42)	4/20 (.20)	ND
PIK3CA WT	24/48 (0.50)	16/24 (0.67)	10/11 (.91)
PIK3CA H1047R	22/64 (0.34)	18/22 (0.82)	16/16 (1.0)
PIK3CA E545K	27/72 (0.38)	24/27 (0.89)	22/22 (1.0)
Clone HR-2	9/24 (.38)	6/9 (.67)	5/6 (.83)
Clone EK-3	9/24 (.38)	7/9 (.78)	1/6 (.17)*

ND – Not determined; * Cells senesced before enough could be harvested for analysis

Table S1, related to Figure 3. Correlation coefficients for various parameter pairings.

Asynchronously growing E545K cells were harvested 24h, 48h, 72h, and 96h after initial plating. Cells were stained with anti-pAKT S473 and anti-HA antibodies and propidium iodide (PI) to monitor DNA content. Cells were analyzed by flow cytometry and the raw data from >10,000 cells/sample were collected for the following parameters: p110α protein, pAKT status, DNA content (PI), cell size (FSC), cell granularity (SSC). The correlation coefficients (R^2 value) for the indicated parameter pairings were calculated, demonstrating that p110α protein level-pAKT status is the only parameter pair with a strong correlation.

Table S2, related to Figure 5. Statistics from the generation of clonal populations. Single cell clones were derived from uninfected MCF10A, pooled wildtype p110α-expressing, pooled mutant p110α -expressing, and mutant clonal parental populations.

Supplemental Methods

Preparation of cells for flow cytometry

Cells were treated as described in Figure Legends. Cells were then washed once with PBS and gently lifted from the plate using a cell scraper with a flexible rubber-like tip (Sarstedt) in 1mL PBS. Cells were briefly triturated with a pipette to obtain a single-cell suspension and immediately fixed by adding PFA to a final concentration of 3.7%. Cells were rocked at room temperature for 10 minutes, spun down and transferred to 5mL polypropylene tubes. Cells were then permeabilized by adding 3mL 100% cold methanol drop-wise while vortexing at medium speed. Tubes were then transferred to ice for >1h or stored at -20°C for up to two weeks before antibody staining.

For staining, cells were washed twice with 3mL staining buffer (0.5% BSA + 0.02% sodium azide in PBS) and rehydrated by 10 minutes incubation at room temperature in staining buffer after each wash. Approximately $1x10^6$ cells were stained per sample in a total volume of 100uL staining buffer plus antibody cocktail. Cells were labeled for 30-60 minutes at room temperature in the dark. Cells were washed twice in staining buffer and stained with secondary antibodies if necessary. Cells were then resuspended in PBS and analyzed on a BD LSR II instrument (BD Biosciences). Data was analyzed with BD FACSDiva software (BD Biosciences), FlowJo software (Tree Star) and Cytobank. Gates are delineated by negative controls (no EGF or wortmannin treatment) in the case of pAKT plots. In HA-p110 plots, gates are set in regions where it is apparent that there are distinct modes.

Immunofluorescence

Cells were grown on glass coverslips and treated as described in figure legends. Cells were fixed in 3.7% PFA, washed with PBS and permeabilized in 100% cold methanol at -20°C. Cells

were washed and blocked with 1% horse serum in PBS for 30 minutes at room temperature. Primary antibody staining was done for 1h at room temperature followed by two PBS washes and secondary antibody staining for 1h at room temperature in the dark. Antibodies used for immunofluorescence were: anti-pAKT S473 (193H12), anti-pEGFR Y1068 (Cell Signaling); anti-HA.11 (Covance); and various secondary Alexa Fluor dyes (Invitrogen).

Immunoblotting

Cells were lysed in RIPA buffer (50mM Tris pH 7.4, 150mM NaCl, 2mM EDTA, 1% NP-40, 0.1% SDS, 0.4% sodium deoxycholate) supplemented with leupeptin (4μg/mL), aprotinin (4μg/mL), pepstatin (4μg/mL), PMSF (1mM), NaF (50mM), $NaPP_i$ (5mM), β-glycerophosphate (10mM), Na_3VO_4 (5mM) and DTT (0.5mM). Lysates were cleared by centrifugation at 14,000 x *g* for 10 minutes at 4°C, and the supernatants were subjected to SDS-PAGE and transferred to polyvinylidene difluoride membranes. Immunoblotting was performed with the following antibodies: anti-HA.11 (Covance), anti-p110α (BD Transduction Laboratories), anti-p85α (Upstate Biotechnology), anti-pAKT S473 (Cell Signaling) and anti-β-actin (Abcam).

Immunohistochemistry

MMTV-Cre; BRCA1 flox/flox; p53+/- mice were bred and maintained in accordance with Beth Israel Deaconess Medical Center IACUC guidelines. Tumors were fixed in SafeFix II solution (Fisher Scientific) and paraffin embedded. Immunohistochemical staining with anti-pAKT S473 (IHC specific) (Cell Signaling) was performed according to the antibody manufacturer's recommendations with the following exceptions: antigen unmasking was done in citrate buffer at a sub-boiling temperature for 20 minutes; and PBST was used as the wash buffer.

Appendix B

Bibliography and Personnel List

Bibliography

1) Yuan, T.L., and Cantley, L.C. Introduction. Curr Top Microbiol Immunol *346*, 1-7.

2) Yuan, T.L., Wulf, G., Burga, L., and Cantley, L.C. (2011) Cell-to-cell variability in PI3K protein regulates PI3K-AKT pathway activity in cell populations. Curr Biol. ***Accepted.***

3) Yuan, T.L. and Cantley, L.C. Single cell analysis reveals heterogeneous activation of PI3K in cell populations that is regulated by PI3K protein levels and altered in tumor cells bearing *PIK3CA* mutations [abstract]. In Cold Spring Harbor James Watson Cancer Symposium; 2010, April 6-11; Suzhou, China. Cold Spring Harbor (NY). Abstract nr. 102.

Personnel receiving pay from this research effort:

Tina Yuan